

36

# Investigation of Applying Normal Mode Initialization Method to Planetary Stationary Wave Disturbances

by

Yang Niu

B.S. in Meteorology,  
Peking University, Beijing  
(1990)

Submitted to the Department of  
Earth, Atmospheric and Planetary Sciences  
in partial fulfillment of the requirements  
for the degree of

Master of Science in Meteorology

at the

Massachusetts Institute of Technology

May, 1992

©Massachusetts Institute of Technology, 1992

Signature of Author \_\_\_\_\_

Center for Meteorology and Physical Oceanography  
Department of Earth, Atmospheric and Planetary Sciences  
May, 1992

Certified by \_\_\_\_\_

Richard S. Lindzen  
Professor of Meteorology  
Thesis Supervisor

Accepted by \_\_\_\_\_

Thomas Jordan, Head  
Department of Earth, Atmospheric and Planetary Sciences  
Lindgren

MASSACHUSETTS INSTITUTE  
OF TECHNOLOGY  
WITHDRAWN  
MAY 27 1992  
MIT LIBRARIES

Investigation of applying normal mode initialization method  
to planetary stationary wave disturbances

by

**Yang Niu**

submitted to the Department of Earth, Atmospheric and Planetary Sciences  
in May, 1992 in partial fulfillment of the requirements for  
the Degree of Master of Science in Meteorology

## **Abstract**

While the prediction of planetary-scale waves has been studied for many years, skillful prediction has not been achieved yet. Complexity is found in some serious problems such as data initialization, domain of integration, model forcing, physical parameterization, etc.. In this paper the problem of applying normal mode initialization to planetary stationary wave disturbances is investigated.

A linearized baroclinic primitive equation model is explored. The initial field is a calculated topographically forced and radiating stationary wave on a beta plane. However, for the purpose of normal mode initialization an artificial model 'top' is imposed. The emphasis of this paper is to determine whether normal mode initialization can affect the time behavior of the initial stationary wave under this circumstance and the dependence of this result on mean zonal flow. In addition, the effect of the placement of the model top on the accuracy of forecasting the stationary waves is examined.

It is found that the vertical modes for the streamfunction  $\psi'$  and  $v'$  velocity are good representations of the vertical structures of initial fields varying in mean zonal flow. However, for  $u'$  velocity only in westerlies do they look like the original ones. Consequently, the time behavior of the initialized and the noninitialized fields bears resemblance in the regime of westerly mean zonal flows. On the contrary, in the presence of easterlies, the initialized field behaves quite differently from the noninitialized field.

Moreover, it is found that in westerlies both of the noninitialized and the initialized fields behave far from stationary waves. However, in easterlies the time behavior of the noninitialized fields is near stationary.

Thesis supervisor: Richard S. Lindzen

Title: Professor of Meteorology

## Acknowledgements

I wish to thank my advisor, Prof. Richard Lindzen for his guidance, insight and patience throughout the course of this research. I also wish to thank Prof. Randy Dole for his helpful discussions and suggestions in the early course of the work.

I would like to thank many of my fellow students for their friendship, encouragement and assistance. Special thanks goes to Michael Morgan for his advice and correcting some parts of the manuscript. Other students, Daniel Reilly, Nilton Renno, Dezheng Sun, Shuntai Zhou, Chun-Chieh Wu and Dennis Boccippio also deserve considerable thanks. Additionally I thank Jane McNabb at CMPO headquarter and Cindy Hanes at EAPS graduate office for their kindness and help in my graduate life at M.I.T.. I'd also like to thank Diana Spiegel for her assistance in using the computational facilities at CMPO.

And last I gratefully thank my host family Mr. and Mrs. Wollman and my good friend Lynn Smith for their love, care and support, which make me feel home, encouraged and joyful.

# Contents

<b>1</b>	<b>Introduction</b>	<b>6</b>
<b>2</b>	<b>Initial forced stationary wave solution</b>	<b>8</b>
2.1	The horizontal structure of the stationary wave . . . . .	10
2.2	The vertical structure of the stationary wave . . . . .	12
<b>3</b>	<b>Normal mode initialization</b>	<b>14</b>
3.1	Normal modes . . . . .	14
3.2	Normal mode initialization . . . . .	18
<b>4</b>	<b>Model description</b>	<b>19</b>
<b>5</b>	<b>Results</b>	<b>24</b>
5.1	The comparison of the initial stationary wave solution and the model stationary wave response . . . . .	24
5.2	Normal mode initialization . . . . .	27
5.3	Time behavior . . . . .	35
<b>6</b>	<b>Discussion</b>	<b>47</b>
6.1	The effect of model lid on initialization . . . . .	47
6.2	The sensitivity of initialization to mean zonal flows . . . . .	52
6.3	The role of vertical wind shear . . . . .	53
6.4	The departure of the evolution of the stationary wave from its initial state . . . . .	62

<b>7 Conclusion</b>	<b>67</b>
<b>8 References</b>	<b>68</b>

# 1 Introduction

Normal mode initialization(NMI) attempts to suppress forecast noise by excluding gravity waves from initial data. Normal modes are determined for the system, and the coefficients in the normal mode expansion are determined from independent initial values of all variables. Since normal mode initialization was first introduced by Dickinson and Williamson (1972), employing this approach to exclude gravity waves from initial data has been extensively studied and applied in short and medium range numerical weather prediction.

However, questions remain about the relevance of normal modes to realistic flows. One of these concerns is the prediction of planetary waves. Although the theoretical study of Lorenz (1969) suggests that the planetary scales are the most predictable, forecasting experiments indicate that the long waves are predicted less accurately than the synoptic scales. The errors of forecasting planetary waves are suggested by Lambert and Meriless (1978) and Baumhefner and Downey (1978) as due to initial data, numerical formulation, domain of integration or physical parameterization. Moreover, Daley and Williamson (1981) suggested that the above first three reasons can all result in the excitation of large-scale free Rossby waves. The purpose of the present paper is to investigate the impact of normal mode initialization on the prediction of stationary planetary waves.

The initial field is a calculated stationary wave on a beta plane in the presence of topography. The stationary wave is obtained for an atmosphere

with no top and hence no complete set of discrete normal modes. One of the critical issues is to evaluate the validity of the application of NMI to the stationary planetary wave if an artificial top is imposed for the purpose of obtaining normal modes. For example, are the initialized fields  $(\psi', u', v')$  good representations of the original ones?

Secondly, the linearized baroclinic primitive model is employed in our test. As a rigid top is imposed in the model, the topographically forced stationary wave response of the model is different from the initial calculated stationary wave with radiation condition. The difference field is expected to travel with the phase speed of free Rossby wave. It was found by Lindzen, Farrell and Jacqmin (1982) that interference can occur between coexisting stationary wave and Rossby wave with the same horizontal wavenumber but different phase speeds. In addition, in our baroclinic primitive model, the traveling Rossby wave may propagate upward. Therefore, the focus of the paper is to test whether the initialization can make a difference in the time behavior of the initial stationary waves in our model.

Furthermore, attention is paid to how the NMI is affected by mean zonal flow, which primarily determines the propagation properties of planetary waves. It was first found by Charney and Drazin (1961) that energy is trapped in the region where zonal winds are easterlies or sufficiently strong westerlies. We propose to examine the sensitivity of NMI to different mean zonal flows.

In addition, the time behaviors of the initial stationary waves from with a



model lid and without a model lid are compared. One advantage of choosing stationary waves as initial fields is that stationary waves do not change at all in nature, and so the solutions from without a lid are already known. When a model lid is imposed, spurious Rossby waves are excited and so the time behaviors of the initial fields are expected different from stationary waves. Therefore, we wish to determine to what extent the spurious Rossby waves contribute to the errors of forecasting the stationary waves.

Finally, to assess the effect of the more realistic flows of easterlies and westerlies together, some simple cases of zonal mean flow with shear are tested.

## 2 Initial forced stationary wave solution

We are concerned with planetary wave disturbances whose horizontal wavelength is comparable in size with the earth's radius and whose doppler shifted period is large compared with the period of the earth's rotation. Such disturbances are therefore both hydrostatic and quasi-geostrophic. The initial field is a topographically forced stationary planetary wave on a  $\beta$ -plane. The perturbation is assumed to be around the basic state, which is isothermal and has dry static stability  $N^2$ . The mean zonal flow of the basic state satisfies the geostrophic relation with the pressure of the basic state.

Let

$$u = \bar{u} + u', v = v', w = w', p = \bar{p}(y, z) + p', \rho = \bar{\rho}(y, z) + \rho', T = \bar{T} + T'$$

where prime denotes perturbation.  $\bar{P}(y, z)$  and  $\bar{\rho}(y, z)$  exponentially decay with  $z$  with a scale height  $H$ .

Linearized perturbation equations are:

$$\bar{u} \frac{\partial u'}{\partial x} - (f_0 + \beta y)v' = -\frac{1}{\bar{\rho}} \frac{\partial p'}{\partial x} \quad (1)$$

$$\bar{u} \frac{\partial v'}{\partial x} + (f_0 + \beta y)u' = -\frac{1}{\bar{\rho}} \frac{\partial p'}{\partial y} \quad (2)$$

$$\bar{u} \frac{\partial \rho'}{\partial x} + \bar{\rho} \left( \frac{\partial u'}{\partial x} + \frac{\partial v'}{\partial y} \right) + \frac{\partial \bar{\rho} w'}{\partial z} = 0 \quad (3)$$

$$\frac{\partial p' / \bar{\rho}}{\partial z} = g \frac{T'}{\bar{T}} \quad (4)$$

$$\bar{u} \frac{\partial T'}{\partial x} - \frac{\bar{u}}{c_p \bar{\rho}} \frac{\partial p'}{\partial x} + w' \left( \frac{\partial \bar{T}}{\partial z} + \frac{g}{c_p} \right) = 0 \quad (5)$$

$$\frac{p'}{\bar{p}} = \frac{\rho'}{\bar{\rho}} + \frac{T'}{\bar{T}} \quad (6)$$

where  $\frac{g}{\bar{T}} \left( \frac{\partial \bar{T}}{\partial z} + \frac{g}{c_p} \right) = N^2$  is Brunt-Vaisälä frequency and  $c_p$  is heat capacity.

Since  $\bar{P}$  satisfies  $\frac{\partial \bar{p}}{\partial y} = -f_0 \bar{\rho} \bar{u}$  and  $\bar{T}$  is constant,  $\bar{\rho}$  satisfies  $\frac{\partial \bar{\rho}}{\partial y} = -\frac{f_0 \bar{u}}{RT} \bar{\rho}$ . However, we do not include  $v' \frac{\partial \bar{\rho}}{\partial y}$  term in continuity equation (3). This is because we compared the magnitude of  $v' \frac{\partial \ln \bar{\rho}}{\partial y}$  with that of  $w' \frac{\partial \ln \bar{\rho}}{\partial z}$  and found that the magnitude of  $\frac{\partial \ln \bar{\rho}}{\partial y}$  is about 4 order smaller than the magnitude of  $\frac{\partial \ln \bar{\rho}}{\partial z}$ , while  $v'$  is only about 2 order larger than  $w'$ .

Let  $\psi'$  to be streamfunction:

$$\psi' = \frac{p'}{f_0 \bar{\rho}} \quad (7)$$

We seek perturbations with independent wave form components of the form of a product of some separable functions of  $x$ ,  $y$  and  $z$ , namely:

$$\psi' = \text{Re}[e^{ikx} \psi'_1(y) \psi'_2(z)] \quad (8)$$

So horizontal and vertical equations are separated as:

$$ik\bar{u}u' - (f_0 + \beta y)v' = -ikf_0\psi'_1 \quad (9)$$

$$ik\bar{u}v' + (f_0 + \beta y)u' = -f_0\frac{\partial\psi'_1}{\partial y} \quad (10)$$

$$iku' + \frac{\partial v'}{\partial y} = -\frac{if_0k\bar{u}}{gh_n}\psi'_1 \quad (11)$$

and

$$-\frac{ik\bar{u}f_0}{g\bar{\rho}}\frac{\partial\bar{\rho}\psi'_2}{\partial z} + \frac{1}{\bar{\rho}}\frac{\partial\bar{\rho}w'}{\partial z} = \frac{ik\bar{u}f_0}{gh_n}\psi'_2 \quad (12)$$

$$f_0\frac{\partial\psi'_2}{\partial z} = g\frac{T'}{\bar{T}} \quad (13)$$

$$ik\bar{u}T' - \frac{ik\bar{u}f_0}{c_p}\psi'_2 + \frac{\bar{T}N^2}{g}w' = 0 \quad (14)$$

where  $h_n$  is the equivalent depth.

The horizontal and vertical structures of the stationary wave are resolved by solving the horizontal equations(9)-(11) and vertical equations(12)-(14) respectively satisfying their own boundary conditions.

## 2.1 The horizontal structure of the stationary wave

Our geometry consists in a channel centered at the latitude of  $45^\circ\text{N}$ . The width of the channel is comparable to the radius of the earth. Using this condition, we can solve the eigenvalue-eigenfunction problem of the stationary solution.

The eigenvalue is found by solving the horizontal equations(9)-(11). The boundary conditions are:

at  $y=0$  and  $y=L$  :

$$v' = 0 \quad (15)$$

or equivalently:

$$\frac{\partial \psi'_1}{\partial y} - \frac{f_0}{\bar{u}} \psi'_1 = 0 \quad (16)$$

Solving  $u'$  and  $v'$  from equations(9)-(10) and substituting them into equation(11), yields:

$$\frac{\partial^2 \psi'_1}{\partial y^2} + \left( \frac{(k\bar{u})^2 - f_0^2}{gh_n} + \frac{\beta}{\bar{u}} - k^2 \right) \psi'_1 = 0 \quad (17)$$

Let:

$$l_n^2 = \frac{(k\bar{u})^2 - f_0^2}{gh_n} + \frac{\beta}{\bar{u}} - k^2 \quad (18)$$

the solution to the equation(17) is:

$$\psi'_1(y) = \sin l_n y + A_n \cos l_n y \quad (19)$$

satisfying the restriction(16). So the  $l_n$  and  $A_n$  are found:

$$l_n = \frac{n\pi}{L}, A_n = \frac{l_n \bar{u}}{f_0} \quad (20)$$

Correspondingly, from equation(18) the equivalent depth  $h_n$  is:

$$gh_n = \frac{f_0^2 - (k\bar{u})^2}{\frac{\beta}{\bar{u}} - k^2 - l_n^2} \quad (21)$$

Then  $u'$  and  $v'$  are solved from equations(9)-(10):

$$u'(y) = \frac{f_0 [k^2 \bar{u} \psi'_1(y) - (f_0 + \beta y) \frac{\partial \psi'_1(y)}{\partial y}]}{(f_0 + \beta y)^2 - (k\bar{u})^2} \quad (22)$$

$$v'(y) = \frac{f_0[ik(f_0 + \beta y)\psi'_1(y) - ik\bar{u}\frac{\partial\psi'_1(y)}{\partial y}]}{(f_0 + \beta y)^2 - (k\bar{u})^2} \quad (23)$$

## 2.2 The vertical structure of the stationary wave

Having found the eigenvalue of the problem, we can resolve the vertical structure of the stationary wave by solving equations(12)-(14). Eliminate  $T'$  and  $w'$  from equations(13)-(14) and substitute them into equation(12), yield:

$$\frac{\partial^2\psi'_2}{\partial z^2} - \left(\frac{1}{H} + \frac{g}{Tc_p} - \frac{N^2}{g}\right)\frac{\partial\psi'_2}{\partial z} - \left(\frac{N^2}{gH} - \frac{g}{HTc_p} - \frac{N^2}{gh_n}\right)\psi'_2 = 0 \quad (24)$$

where  $h_n$  is obtained from the eigenvalue solution equation(21). The vertical boundary conditions are:

at  $z=0$ :

$$\frac{ik\bar{u}f_0}{N^2}\left(\frac{\partial}{\partial z} - \frac{g}{Tc_p}\right)\psi'_2 = -w'_s \quad (25)$$

at  $z=\text{top}$ :

$$\frac{ik\bar{u}f_0}{N^2}\left(\frac{\partial}{\partial z} - \frac{g}{Tc_p}\right)\psi'_2 = 0 \quad (26)$$

The  $w'_s$  appearing on the right hand side of equation(25) is the surface forcing:

$$w'_s = ik\bar{u}\eta_s \quad (27)$$

where  $\eta_s$  is the height of topography.

We noticed that the coefficients of  $\psi'_2$  and  $\frac{\partial\psi'_2}{\partial z}$  in equation(24) and in the boundary condition equations(25)-(26) are slightly different from those in the classical equations of Charney and Drazin(1961). This is because we added  $\bar{u}\frac{\partial\rho'}{\partial x}$  term in continuity equation(3) and  $-\frac{\bar{u}}{c_p\bar{\rho}}\frac{\partial p'}{\partial x}$  term in thermal equation(5)

as we considered the stationary equations as compatible as possible to the time dependent equations used later. We also calculated that the magnitudes of the additional terms in equations(24),(25) and (26) are about 1 to 2 order less than those of the original terms in Charney and Drazin. Therefore, the change we made here does not matter.

The equation(24) can be transformed into canonical form:

$$\frac{d^2\Psi}{dz^2} + (\alpha_1 - \frac{\alpha_2^2}{4})\Psi = 0 \quad (28)$$

by setting  $\alpha_1$  and  $\alpha_2$  to be the coefficients of  $\psi'_2$  and  $\frac{\partial\psi'_2}{\partial z}$  respectively in equation(24):

$$\alpha_1 = -\left(\frac{N^2}{gH} - \frac{g}{HTc_p} - \frac{N^2}{gh_n}\right) \quad (29)$$

$$\alpha_2 = -\left(\frac{1}{H} + \frac{g}{Tc_p} - \frac{N^2}{g}\right) \quad (30)$$

and

$$\Psi = \psi'_2 e^{\frac{\alpha_2}{2}z} \quad (31)$$

It's easy to see that the propagating property of the solution to equation(28) depends on the sign of  $(\alpha_1 - \frac{\alpha_2^2}{4})$ . Here we define

$$\gamma^2 = \alpha_1 - \frac{\alpha_2^2}{4} \quad (32)$$

$\gamma^2$  is a function of mean zonal flow  $\bar{u}$ . In weak westerlies  $\gamma^2 > 0$ , and the stationary wave will propagate, while in easterlies or sufficiently strong westerlies  $\gamma^2 < 0$ , and it will be trapped.

Satisfying the boundary conditions(25)-(26), we obtain the vertical structure solution  $\psi'_2$ : (for simplicity, use  $\gamma = |\gamma| > 0$ )

For propagating wave ( $\gamma^2 > 0$ ):

$$\psi'_2(z) = -\frac{N^2\eta_s}{f_0(-i\gamma - \frac{\alpha_2}{2} - \frac{g}{T_{cp}})} e^{(-i\gamma - \frac{\alpha_2}{2})z} \quad (33)$$

For trapped wave ( $\gamma^2 < 0$ ):

$$\psi'_2(z) = -\frac{N^2\eta_s}{f_0(-\gamma - \frac{\alpha_2}{2} - \frac{g}{T_{cp}})} e^{(-\gamma - \frac{\alpha_2}{2})z} \quad (34)$$

Therefore, the initial forced stationary wave solution is found:

For propagating wave ( $\gamma^2 > 0$ ):

$$\psi' = \text{Re}[A_p e^{ikx} (\sin l_n y + A_n \cos l_n y) e^{(-i\gamma - \frac{\alpha_2}{2})z}] \quad (35)$$

where

$$A_p = -\frac{N^2\eta_s}{f_0(-i\gamma - \frac{\alpha_2}{2} - \frac{g}{T_{cp}})} \quad (36)$$

For trapped wave ( $\gamma^2 < 0$ ):

$$\psi' = \text{Re}[A_t e^{ikx} (\sin l_n y + A_n \cos l_n y) e^{(-\gamma - \frac{\alpha_2}{2})z}] \quad (37)$$

where

$$A_t = -\frac{N^2\eta_s}{f_0(-\gamma - \frac{\alpha_2}{2} - \frac{g}{T_{cp}})} \quad (38)$$

## 3 Normal mode initialization

### 3.1 Normal modes

First, we are going to find the normal modes of atmosphere. Assume the atmosphere is restricted between two vertical boundaries with depth of D.

The vertical dependent equations are:

$$-\frac{i\omega f_0}{gh_n}\psi_n' + \frac{1}{\bar{\rho}}\frac{\partial \bar{\rho} w_n'}{\partial z} = 0 \quad (39)$$

$$i\omega \frac{\partial \psi_n'}{\partial z} + \frac{N^2}{f_0} w_n' = 0 \quad (40)$$

where  $\omega$  is frequency and  $h_n$  is the equivalent depth of mode. Eliminating  $\psi'$  from equation(39) and substituting it into equation(40), yields:

$$\frac{\partial^2 w_n^*}{\partial z^2} + \left(\frac{N^2}{gh_n} - \frac{1}{4H^2}\right)w_n^* = 0 \quad (41)$$

where

$$w^* = w' e^{-\frac{z}{2H}} \quad (42)$$

To find normal modes is to solve the following eigenvalue-eigenfunction problem:

$$\frac{\partial^2 w^*}{\partial z^2} + m^2 w^* = 0 \quad (43)$$

where

$$m^2 = \frac{N^2}{gh_n} - \frac{1}{4H^2} \quad (44)$$

satisfying the boundary conditions:

at  $z=0$  and  $z=D$ :

$$w^* = w = 0 \quad (45)$$

or equivalently

$$\frac{\partial \psi'}{\partial z} = 0 \quad (46)$$

So the solution to equation(43) is:

$$w^* = \sin mz \quad (47)$$



and

$$\psi' = \cos mz \quad (48)$$

where  $m = \frac{p\pi}{D}$ ,  $p=0,1,2,\dots$

In order to do normal mode initialization, we then project the initial stationary wave into normal modes. Set:

$$\psi = \text{Re}\left[\sum_{m=0}^{\infty} \psi_m \cos mz\right] \quad (49)$$

$$u = \text{Re}\left[\sum_{m=0}^{\infty} u_m \cos mz\right] \quad (50)$$

$$v = \text{Re}\left[\sum_{m=0}^{\infty} v_m \cos mz\right] \quad (51)$$

the coefficients of normal modes are determined by Fourier expansion of the stationary wave solutions(35)-(38).

For propagating wave ( $\gamma^2 > 0$ ) :

$$\psi'_0 = \frac{A_p}{(-i\gamma - \frac{\alpha_2}{2})D} (e^{(-i\gamma - \frac{\alpha_2}{2})D} - 1) \psi'_1(y) e^{ikx} \quad (52)$$

$$u'_0 = \frac{A_p}{(-i\gamma - \frac{\alpha_2}{2})D} (e^{(-i\gamma - \frac{\alpha_2}{2})D} - 1) u'(y) e^{ikx} \quad (53)$$

$$v'_0 = \frac{A_p}{(-i\gamma - \frac{\alpha_2}{2})D} (e^{(-i\gamma - \frac{\alpha_2}{2})D} - 1) v'(y) e^{ikx}, \quad m = 0 \quad (54)$$

and

$$\psi'_m = \frac{2}{D} \frac{(-i\gamma - \frac{\alpha_2}{2})A_p}{m^2 + (-i\gamma - \frac{\alpha_2}{2})^2} ((-1)^p e^{(-i\gamma - \frac{\alpha_2}{2})D} - 1) \psi'_1(y) e^{ikx} \quad (55)$$

$$u'_m = \frac{2}{D} \frac{(-i\gamma - \frac{\alpha_2}{2})A_p}{m^2 + (-i\gamma - \frac{\alpha_2}{2})^2} ((-1)^p e^{(-i\gamma - \frac{\alpha_2}{2})D} - 1) u'(y) e^{ikx} \quad (56)$$

$$v'_m = \frac{2}{D} \frac{(-i\gamma - \frac{\alpha_2}{2})A_p}{m^2 + (-i\gamma - \frac{\alpha_2}{2})^2} * ((-1)^p e^{(-i\gamma - \frac{\alpha_2}{2})D} - 1)v'(y)e^{ikx},$$

$$m = \frac{p\pi}{D}, p = 1, 2, 3... \quad (57)$$

where  $A_p = -\frac{N^2\eta_s}{f_0(-i\gamma - \frac{\alpha_2}{2} - \frac{g}{Tc_p})}$

For trapped wave ( $\gamma^2 < 0$ ):

$$\psi'_0 = \frac{A_t}{(-\gamma - \frac{\alpha_2}{2})D} (e^{(-\gamma - \frac{\alpha_2}{2})D} - 1)\psi'_1(y)e^{ikx} \quad (58)$$

$$u'_0 = \frac{A_t}{(-\gamma - \frac{\alpha_2}{2})D} (e^{(-\gamma - \frac{\alpha_2}{2})D} - 1)u'(y)e^{ikx} \quad (59)$$

$$v'_0 = \frac{A_t}{(-\gamma - \frac{\alpha_2}{2})D} (e^{(-\gamma - \frac{\alpha_2}{2})D} - 1)v'(y)e^{ikx},$$

$$m = 0 \quad (60)$$

and

$$\psi'_m = \frac{2}{D} \frac{(-\gamma - \frac{\alpha_2}{2})A_t}{m^2 + (-\gamma - \frac{\alpha_2}{2})^2} ((-1)^p e^{(-\gamma - \frac{\alpha_2}{2})D} - 1)\psi'_1(y)e^{ikx} \quad (61)$$

$$u'_m = \frac{2}{D} \frac{(-\gamma - \frac{\alpha_2}{2})A_t}{m^2 + (-\gamma - \frac{\alpha_2}{2})^2} ((-1)^p e^{(-\gamma - \frac{\alpha_2}{2})D} - 1)u'(y)e^{ikx} \quad (62)$$

$$v'_m = \frac{2}{D} \frac{(-\gamma - \frac{\alpha_2}{2})A_t}{m^2 + (-\gamma - \frac{\alpha_2}{2})^2} * ((-1)^p e^{(-\gamma - \frac{\alpha_2}{2})D} - 1)v'(y)e^{ikx},$$

$$m = \frac{p\pi}{D}, p = 1, 2, 3... \quad (63)$$

where  $A_t = -\frac{N^2\eta_s}{f_0(-\gamma - \frac{\alpha_2}{2} - \frac{g}{Tc_p})}$

### 3.2 Normal mode initialization

For normal mode initialization the horizontal dependent equations are linearized around the basic state of rest. Set the perturbation to be the form of  $e^{i(kx-\omega t)}$ , the linearized equations for each vertical tranformation can be written in a matrix form:

$$\omega \begin{bmatrix} u'_m \\ v'_m \\ \frac{f_0}{\sqrt{gh_m}} \psi'_m \end{bmatrix} = \begin{bmatrix} 0 & i(f_0 + \beta y) & k\sqrt{gh_m} \\ -i(f_0 + \beta y) & 0 & -i\sqrt{gh_m} \frac{\partial}{\partial y} \\ k\sqrt{gh_m} & i\sqrt{gh_m} \frac{\partial}{\partial y} & 0 \end{bmatrix} \begin{bmatrix} u'_m \\ v'_m \\ \frac{f_0}{\sqrt{gh_m}} \psi'_m \end{bmatrix} \quad (64)$$

The 3x3 matrix explicitly appearing on the right-hand side of the above matrix equation(64) is Hermitian, so every eigenvalue  $\omega$  of the matrix is real value. The three eigenvalues of the 3x3 matrix are Rossby wave frequency and two gravity wave frequencies.

Since the initial field includes both basic state and perturbation, we need to initialize both of them by NMI. The basic state is geostrophic and independent of x:

$$(f_0 + \beta y)\bar{u} = -f_0 \frac{\partial \bar{\psi}(y)}{\partial y} \quad (65)$$

$$\bar{v} = 0 \quad (66)$$

so the matrix(64) for basic state becomes:

$$\omega \begin{bmatrix} \bar{u} \\ \bar{v} \\ \frac{f_0}{\sqrt{gh_0}} \bar{\psi} \end{bmatrix} = \begin{bmatrix} 0 & i(f_0 + \beta y) & 0 \\ -i(f_0 + \beta y) & 0 & -i\sqrt{gh_0} \frac{\partial}{\partial y} \\ 0 & 0 & 0 \end{bmatrix} \begin{bmatrix} \bar{u} \\ \bar{v} \\ \frac{f_0}{\sqrt{gh_0}} \bar{\psi} \end{bmatrix} \quad (67)$$

The projection of the stationary wave into Rossby wave and gravity waves is:

$$\begin{bmatrix} u'_m \\ v'_m \\ \frac{f_0}{\sqrt{gh_m}}\psi'_m \end{bmatrix} = X \begin{bmatrix} r \\ g \\ g' \end{bmatrix} \quad (68)$$

where  $r$  denotes Rossby wave,  $g$  and  $g'$  denote east and west propagating gravity waves respectively. The matrix  $X$  is composed of the corresponding three eigen-vectors. Therefore, the  $r$ ,  $g$ , and  $g'$  are obtained by inverting the matrix  $X$ :

$$\begin{bmatrix} r \\ g \\ g' \end{bmatrix} = X^{-1} \begin{bmatrix} u'_m \\ v'_m \\ \frac{f_0}{\sqrt{gh_m}}\psi'_m \end{bmatrix} \quad (69)$$

For the purpose of normal mode initialization, the gravity wave component of the initial stationary wave is excluded by setting both  $g$  and  $g'$  to zero, namely:

$$\begin{bmatrix} u'_m \\ v'_m \\ \frac{f_0}{\sqrt{gh_m}}\psi'_m \end{bmatrix} = X \begin{bmatrix} r \\ 0 \\ 0 \end{bmatrix} \quad (70)$$

## 4 Model description

We employ time-dependent linearized baroclinic primitive equation model. The basic state is the same as we used in the initial stationary wave. Namely, isothermal, constant mean zonal flow  $\bar{u}$  and static stability  $N^2$ . The time-

dependent linearized equations are:

$$\frac{\partial u'}{\partial t} + \bar{u} \frac{\partial u'}{\partial x} - (f_0 + \beta y)v' = -\frac{1}{\bar{\rho}} \frac{\partial p'}{\partial x} \quad (71)$$

$$\frac{\partial v'}{\partial t} + \bar{u} \frac{\partial v'}{\partial x} + (f_0 + \beta y)u' = -\frac{1}{\bar{\rho}} \frac{\partial p'}{\partial y} \quad (72)$$

$$\frac{\partial T'}{\partial t} + \bar{u} \frac{\partial T'}{\partial x} - \frac{1}{c_p \bar{\rho}} \frac{\partial p'}{\partial t} - \frac{\bar{u}}{c_p \bar{\rho}} \frac{\partial p'}{\partial x} + \frac{\bar{T} N^2}{g} w' = 0 \quad (73)$$

$$\frac{\partial \rho'}{\partial t} + \bar{u} \frac{\partial \rho'}{\partial x} + \bar{\rho} \left( \frac{\partial u'}{\partial x} + \frac{\partial v'}{\partial y} \right) + \frac{\partial \bar{\rho} w'}{\partial z} = 0 \quad (74)$$

$$\frac{\partial p' / \bar{\rho}}{\partial z} = g \frac{T'}{\bar{T}} \quad (75)$$

$$\frac{p'}{\bar{p}} = \frac{\rho'}{\bar{\rho}} + \frac{T'}{\bar{T}} \quad (76)$$

The horizontal and vertical boundary conditions are the same as we used in obtaining the initial stationary solution except that there is a model 'top' at the height D. Thus, the vertical boundary conditions in our model are:

at  $z=D$ ,

$$w' = 0 \quad (77)$$

at  $z=0$ ,

$$w'_s = ik\bar{u}\eta_s \quad (78)$$

The stationary part of the model can be computed numerically by setting all  $\frac{\partial}{\partial t}$  part in equations(71)-(74) to zero.

As horizontal boundary is satisfied, the solutions to equations(71)-(76) are set to be the form of the product of function of  $(z,t)$  and  $e^{ikx} F(y)$ , where

$F(y)$  is the same as the  $y$ -dependent structure of the initial stationary solutions(19), (22) and (23). Therefore, the time-dependent part of our model is only in vertical modes.

For numerical computation the above time-dependent equations are transformed into prognostic and diagnostic equations:

$$\frac{\partial u'}{\partial t} = -ik\bar{u}u' + (f_0 + \beta y)v' - ikf_0\psi' \quad (79)$$

$$\frac{\partial v'}{\partial t} = -ik\bar{u}v' - (f_0 + \beta y)u' - f_0\frac{\partial\psi'}{\partial y} \quad (80)$$

$$\begin{aligned} \frac{\partial T'}{\partial t} = & -ik\bar{u}T' - \frac{R\bar{T}}{c_v}(iku' + \frac{\partial v'}{\partial y}) \\ & - \frac{R\bar{T}}{c_v}\left(\frac{\partial}{\partial z} - \frac{1}{H}\right)w' - \frac{c_p\bar{T}N^2}{c_v g}w' \end{aligned} \quad (81)$$

$$\begin{aligned} \frac{\partial}{\partial t}(\bar{\rho}_s\psi'_s - \bar{\rho}_t\psi'_t) = & -ik\bar{u}(\bar{\rho}_s\psi'_s - \bar{\rho}_t\psi'_t) - \frac{g}{f_0}\int_s^t \bar{\rho}(iku' + \frac{\partial v'}{\partial y})dz \\ & + \frac{g}{f_0}\bar{\rho}_s w'_s \end{aligned} \quad (82)$$

$$\frac{\partial\psi'}{\partial z} = g\frac{T'}{\bar{T}} \quad (83)$$

$$\begin{aligned} w' = & \frac{f_0}{g}\frac{\partial}{\partial t}\left(\psi' - \frac{\bar{\rho}_t}{\bar{\rho}}\psi'_t\right) + \frac{ik\bar{u}f_0}{g}\left(\psi' - \frac{\bar{\rho}_t}{\bar{\rho}}\psi'_t\right) \\ & + \frac{1}{\bar{\rho}}\int_z^t \bar{\rho}\left(iku' + \frac{\partial v'}{\partial y}\right)dz \end{aligned} \quad (84)$$

where  $\psi' = p'/f_0\bar{\rho}$  and  $H$  is the scale height. The subscripts  $s$  and  $t$  denote the surface and the model top respectively. The tendency equation(82) is obtained by eliminating  $\rho'$  from equations(75)-(76) and substituting it into continuity equation(74), and then integrating the continuity equation from surface to top. The diagnostic vertical velocity is obtained by integrating the same continuity equation from  $z$  to top.

The prognostic equations(79)-(82) are integrated in time using mid-point Euler-backward method. That is: for the first-order differential equation

$$\frac{\partial A}{\partial t} = R \quad (85)$$

where A denotes time-dependent variable and R the right-hand side, the A forwards in one time step after being computed four times:

$$A_{n+1}^* = A_n + R(A_n)\Delta t \quad (86)$$

$$A_{n+1}^{**} = A_n + R(A_{n+1}^*)\Delta t \quad (87)$$

$$A_{n+1}^{***} = A_n + R\left(A_n + \frac{A_{n+1}^{**} - A_n}{2}\right)\Delta t \quad (88)$$

$$A_{n+1} = A_n + R\left(A_n + \frac{A_{n+1}^{***} - A_n}{2}\right)\Delta t \quad (89)$$

where the subscript n denotes time point.

Finite differences are used for vertical direction. Vertical layers and the displacement of all 5 variables  $u', v', T', \psi', w'$  in these layers are sketched in Fig.1.

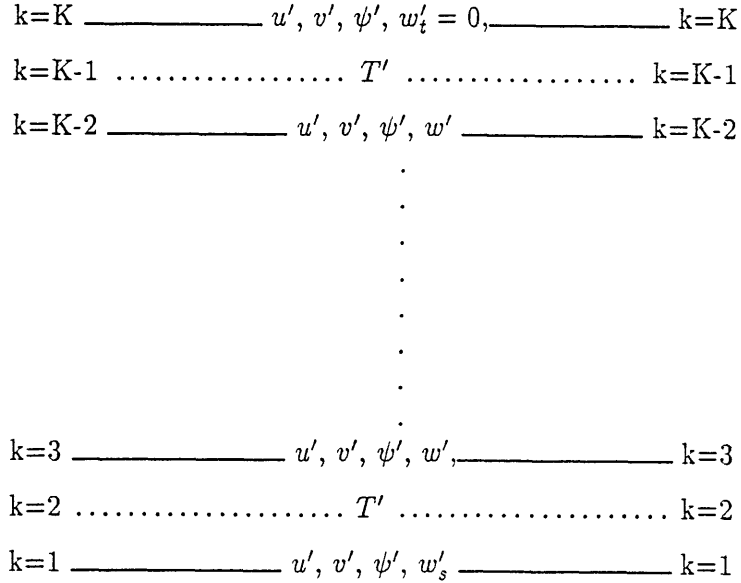


Figure 1: Vertical layers  $k$  and the displacement of variables on these layers.  $k=1$ : the surface,  $k=K$ : the model top

The second-order leap-frog scheme is used to approximate the vertical spatial derivatives. For  $y$  direction the equations(79)-(84) are integrated independently in specified grid points. All the partial differentials  $\frac{\partial}{\partial y}$  appearing on the right-hand side of equations(79)-(84) are the direct derivatives of  $y$ -dependent structure  $\frac{\partial F(y)}{\partial y}$ .



## 5 Results

In this section we present the major results in our test. First we list the parameters used in our model:

model top:  $D = 20.Km$

horizontal wavenumbers:  $k=4.44 * 10^{-7}m^{-1}$ ,  $l=4.8 * 10^{-7}m^{-1}$

scale height:  $H = 7.99Km$

temperature:  $\bar{T} = 273^0K$

static stability:  $N^2 = 4.0 * 10^{-4}sec^{-2}$

the height of topography:  $\eta_s = 1.Km$

$f_0 = 1.03 * 10^{-4}sec^{-1}$

$\beta = 1.6 * 10^{-11}sec^{-1}m^{-1}$

vertical resolution:  $1.Km$

time step:  $3min.$

### 5.1 The comparison of the initial stationary wave solution and the model stationary wave response

The initial stationary wave solution is calculated by using radiation condition on the top, while the model stationary wave is computed by imposing a lid on the top. The vertical structure of these two waves against different mean zonal flows are plotted in Fig.2. It is shown that the initial stationary waves under mean flows of  $\bar{u} = 10.m/s$  and  $\bar{u} = 25.m/s$  are both vertically propagating. Due to the reflection of the model lid the model sta-

tionary responses are different from the initial stationary waves especially in  $\bar{u} = 10.m/s$ . At stronger westerly  $\bar{u} = 45.m/s$  the initial stationary wave is trapped. However, the amplitude of the model stationary wave decreases with height up to 14Km and then increases up to the top. Moreover, in easterlies the initial stationary waves are heavily trapped and they look like the model stationary waves.

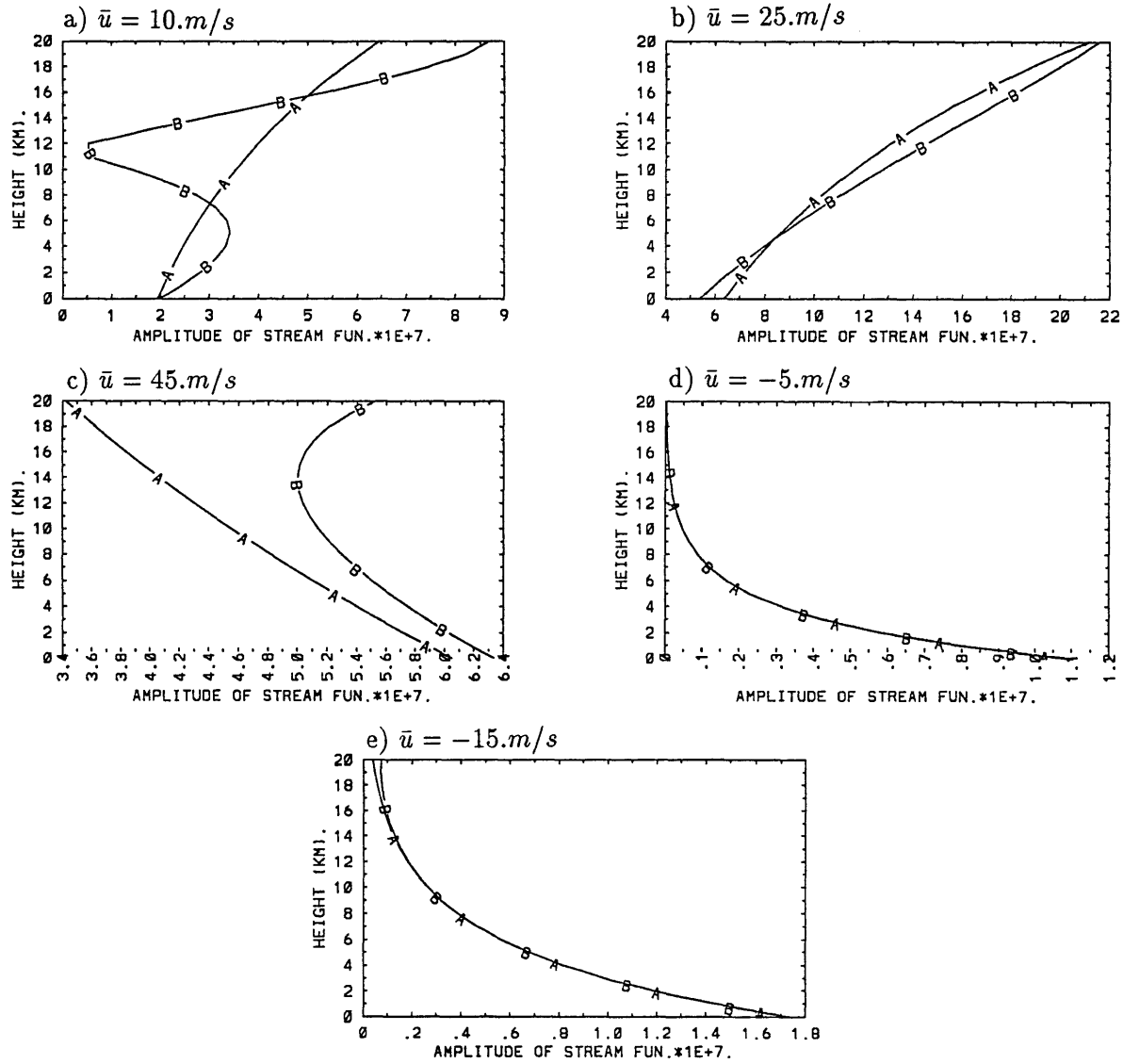


Figure 2: The vertical structure of streamfunction  $\psi'$  in  $m^2/s * 10^7$  of the initial stationary wave with radiation condition (A letter) and the model stationary wave with a lid (B letter) against different mean zonal flows: a)  $\bar{u} = 10. m/s$ , b)  $\bar{u} = 25. m/s$ , c)  $\bar{u} = 45. m/s$ , d)  $\bar{u} = -5. m/s$ , e)  $\bar{u} = -15. m/s$ .

## 5.2 Normal mode initialization

We first initialize the basic state of the initial field. It is found that in varying mean flows ranging from easterlies to westerlies the Rossby wave frequencies are near zero and the projections of the initial field almost completely go into Rossby waves. This result is reasonable as the basic state is geostrophic. We do not show the result here.

The coefficients of the normal modes of the original perturbation fields  $(\psi', u', v')$  and the initialized fields against different mean flows are plotted in Fig.3-Fig.7. Here we only show the results of initialization at  $45^\circ N$ . In addition, since in the cases of  $\bar{u} = 10.m/s$  and  $\bar{u} = 25.m/s$  the stationary waves are propagating, and all the variables are complex values, we plot both of the amplitude and the phase of  $\psi', v'$  and  $u'$ . However, in the other cases the stationary waves are trapped and all the variables are real values, so we only plot the variables themselves.

$$\bar{u} = 10.m/s$$

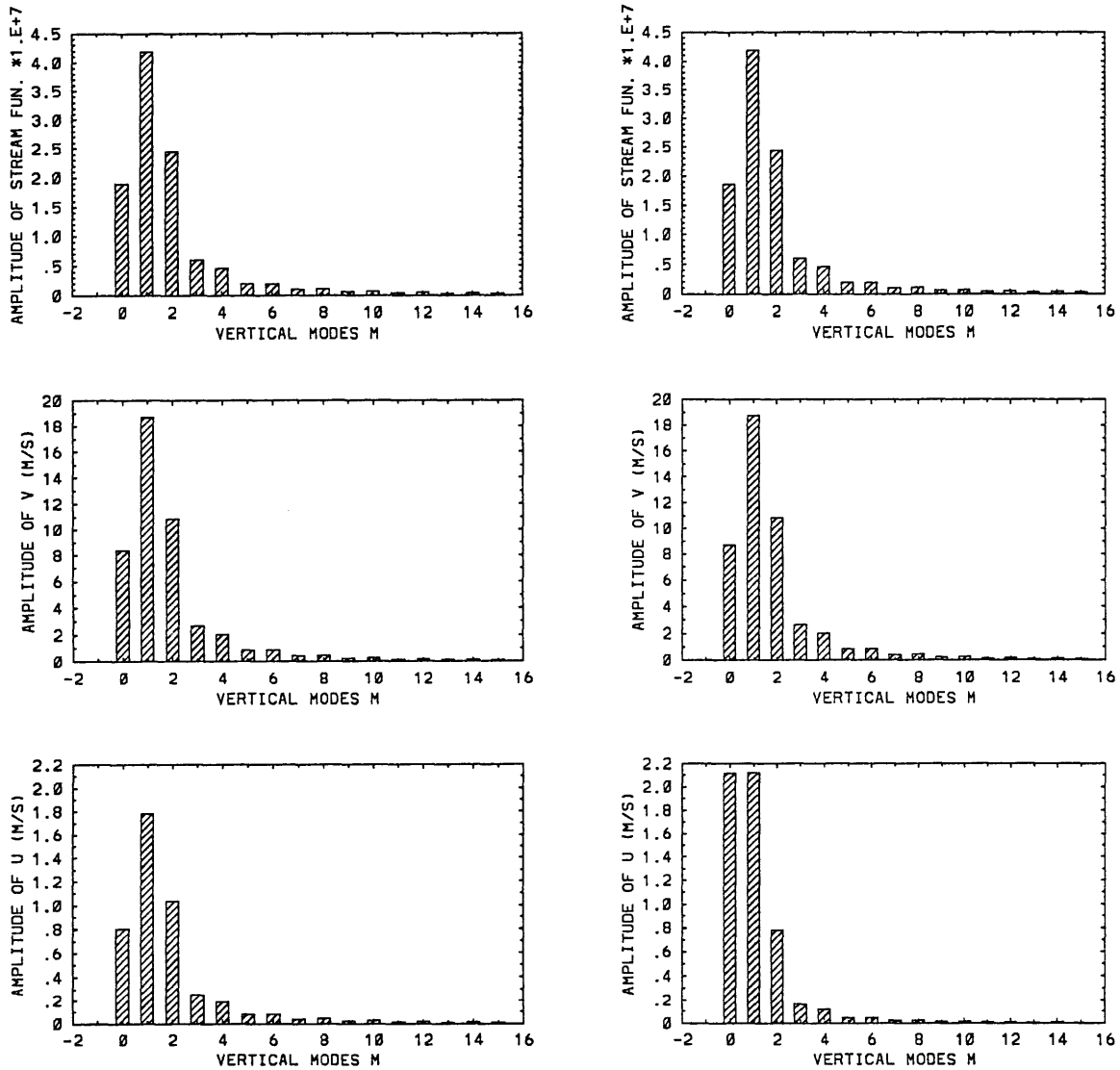


Figure 3(a): The amplitude of streamfunction  $\psi'$  in  $m^2/s * 10^7$ ,  $v'$  and  $u'$  in  $m/s$  versus vertical modes from mode 0 to mode 15 for  $\bar{u} = 10.m/s$ . Left: the noninitialized field, Right: the initialized field.

$$\bar{u} = 10.m/s$$

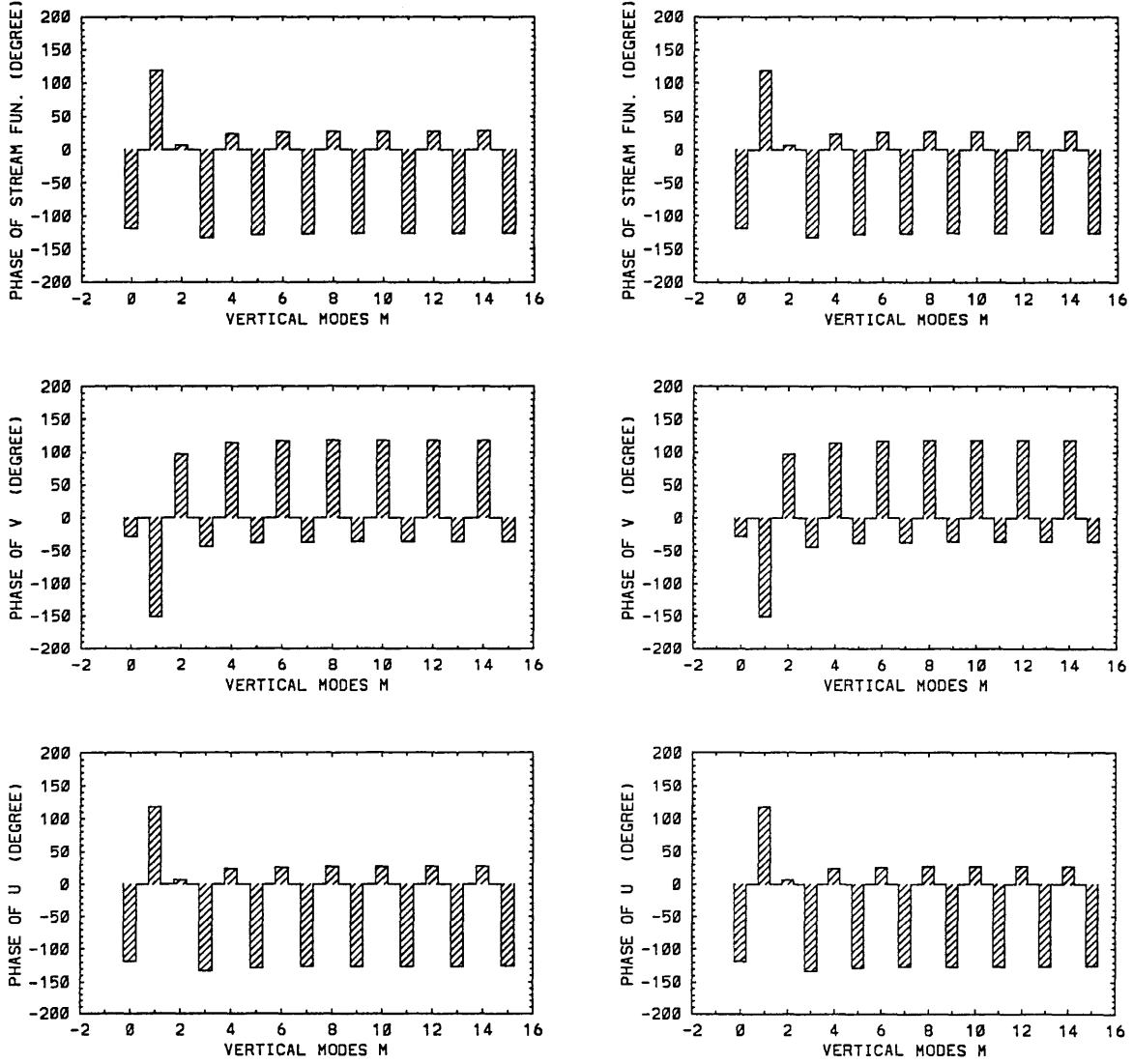


Figure 3(b): The phase of  $\psi'$ ,  $v'$  and  $u'$  in degree versus vertical modes from mode 0 to mode 15 for  $\bar{u} = 10.m/s$ . Left: the noninitialized field, Right: the initialized field.

$$\bar{u} = 25.m/s$$

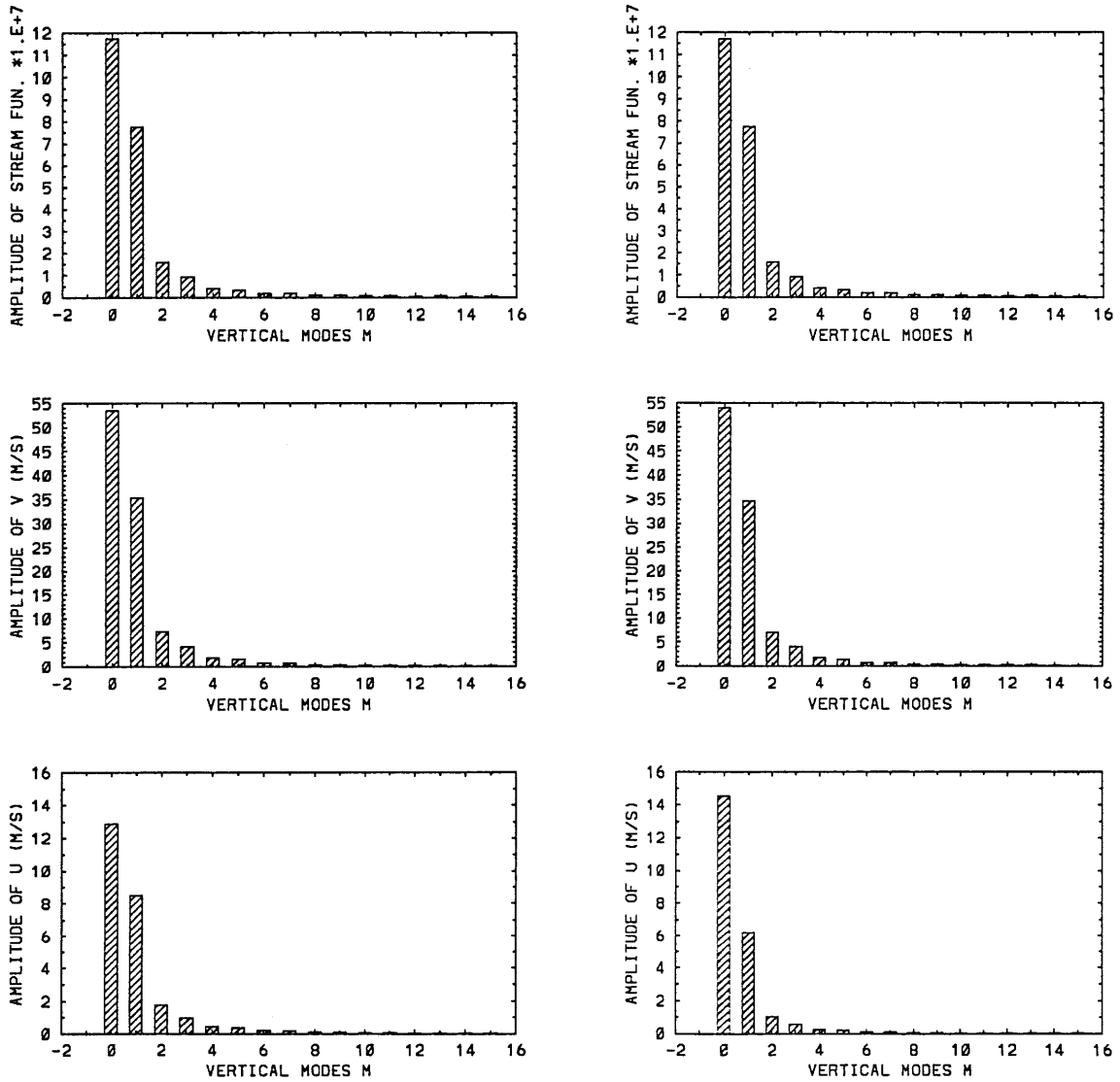


Figure 4(a): As in Figure 3(a) but for  $\bar{u} = 25.m/s$

$$\bar{u} = 25.m/s$$

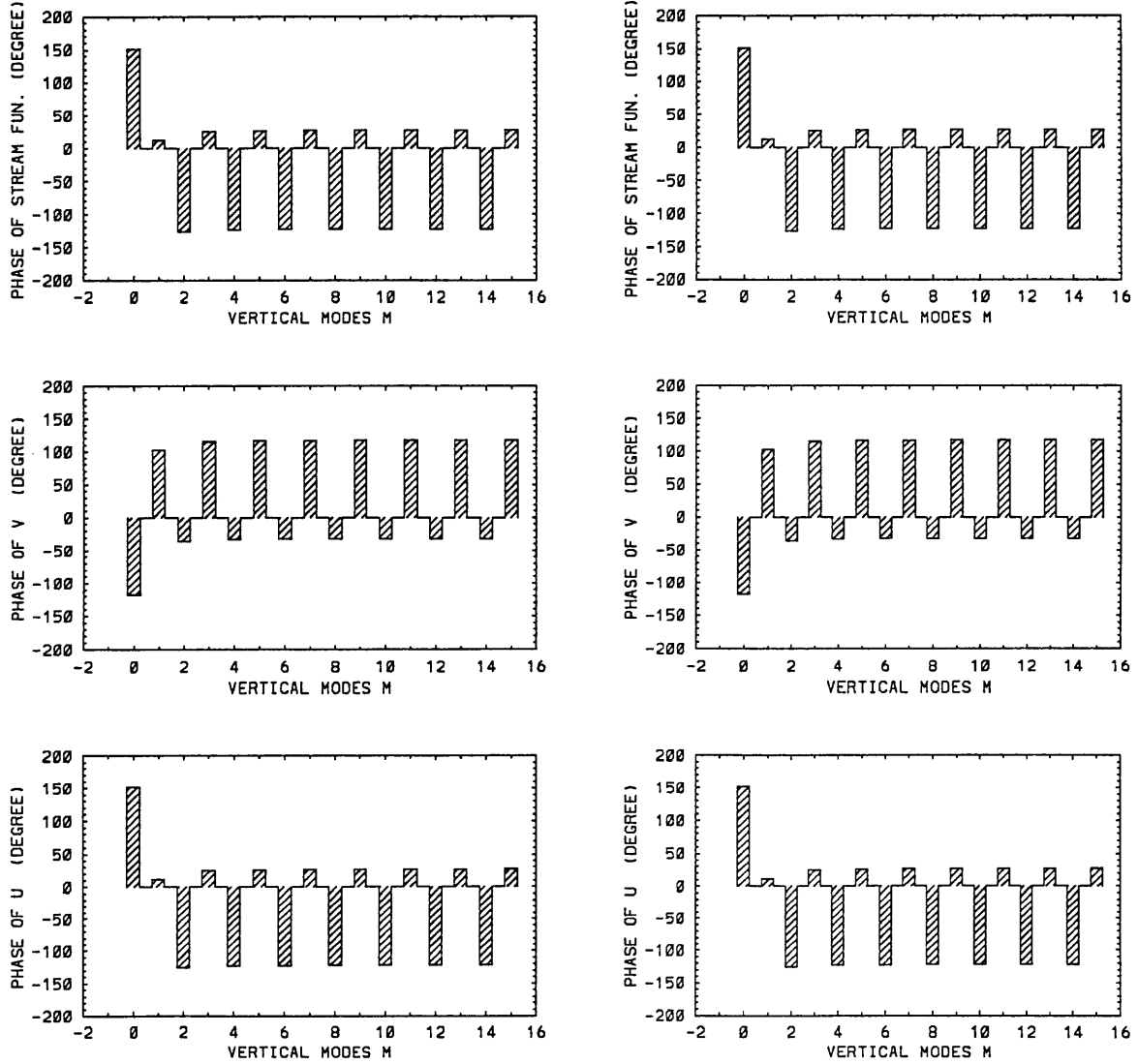


Figure 4(b): As in Figure 3(b) but for  $\bar{u} = 25.m/s$



$$\bar{u} = 45.m/s$$

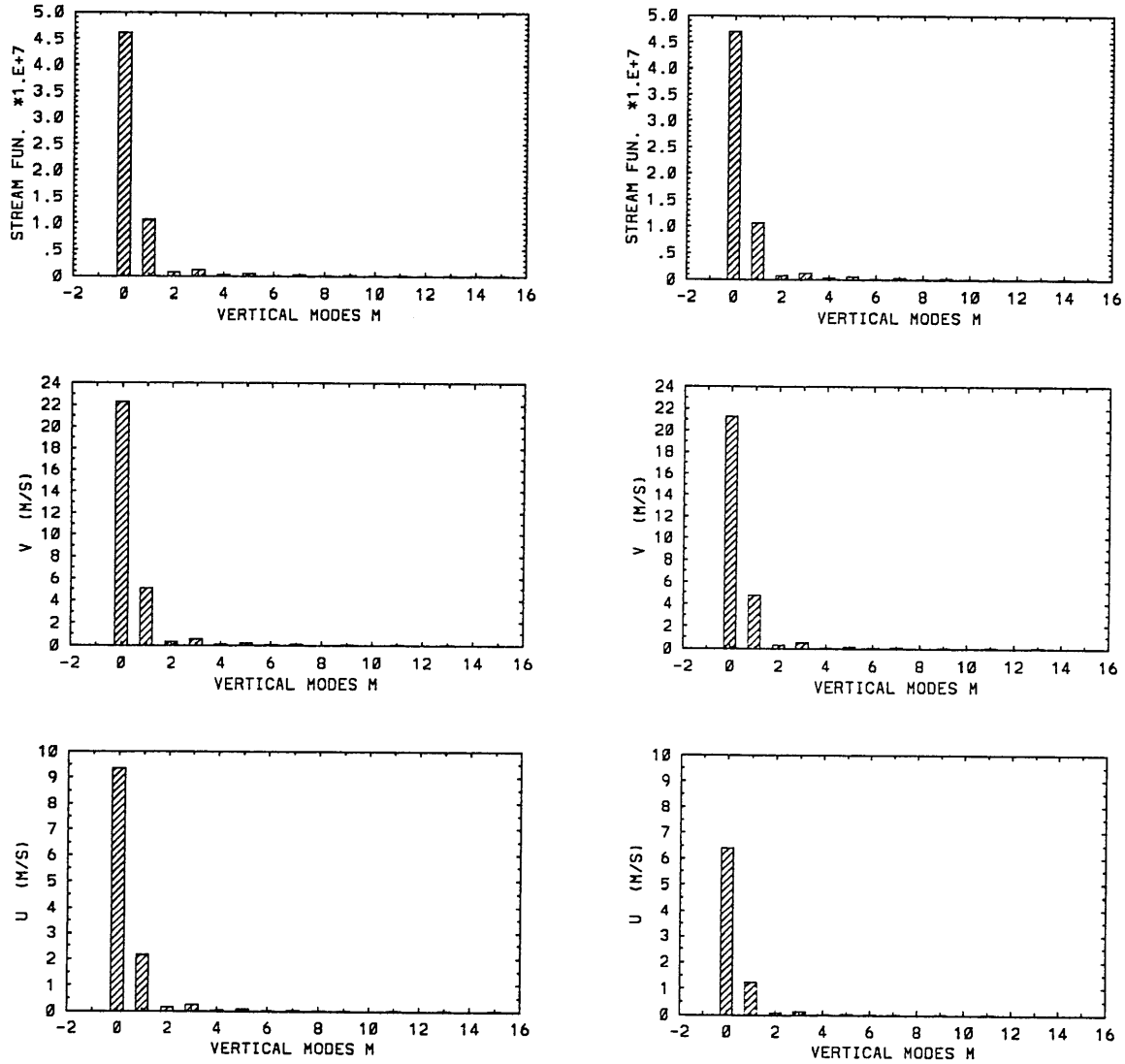


Figure 5: Streamfunction  $\psi'$  in  $m^2/s * 10^7$ ,  $v'$  and  $u'$  in  $m/s$  versus vertical modes from mode 0 to mode 15 for  $\bar{u} = 45.m/s$

$$\bar{u} = -5.m/s$$

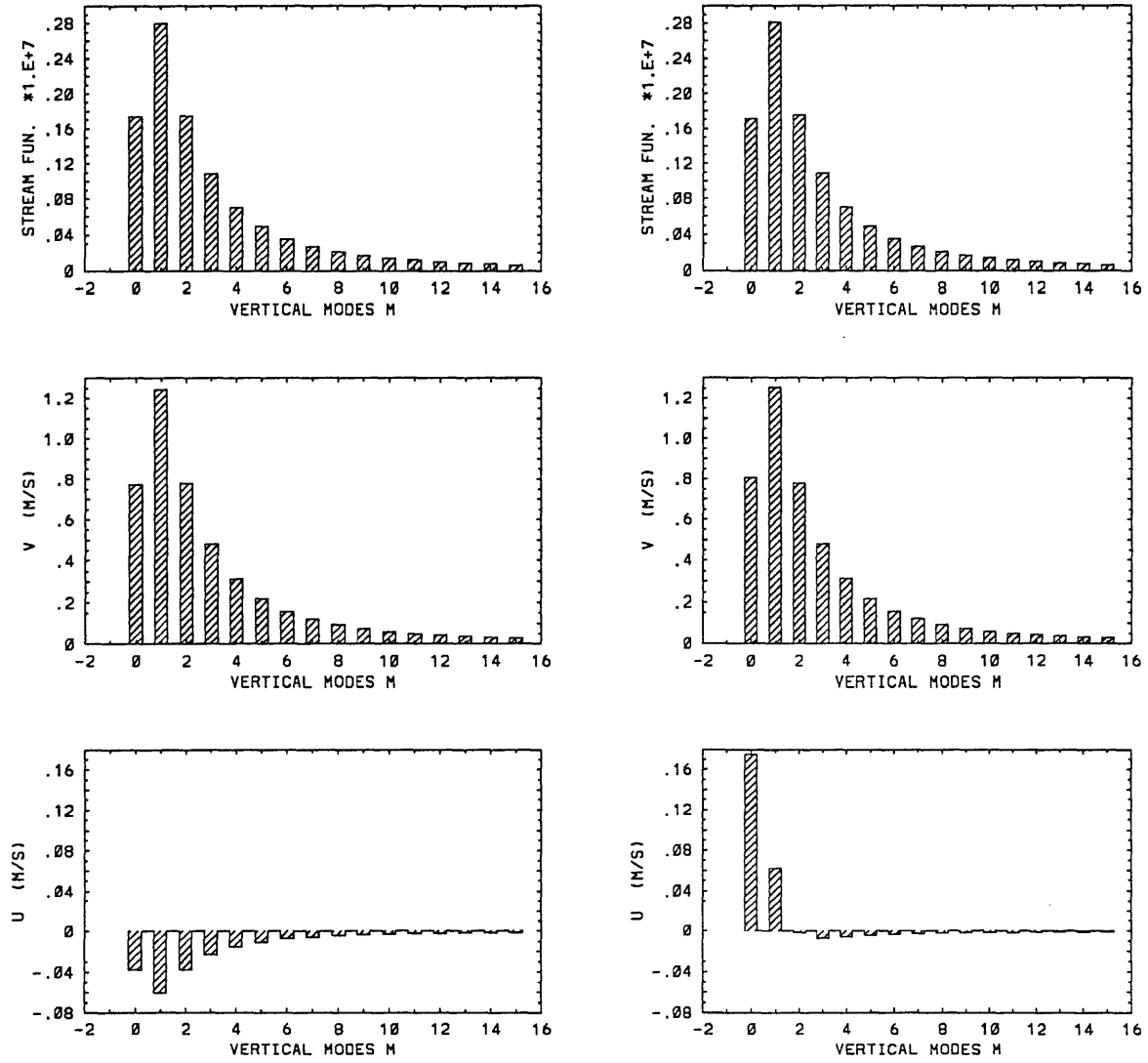


Figure 6: As in Figure 5 but for  $\bar{u} = -5.m/s$

$$\bar{u} = -15.m/s$$

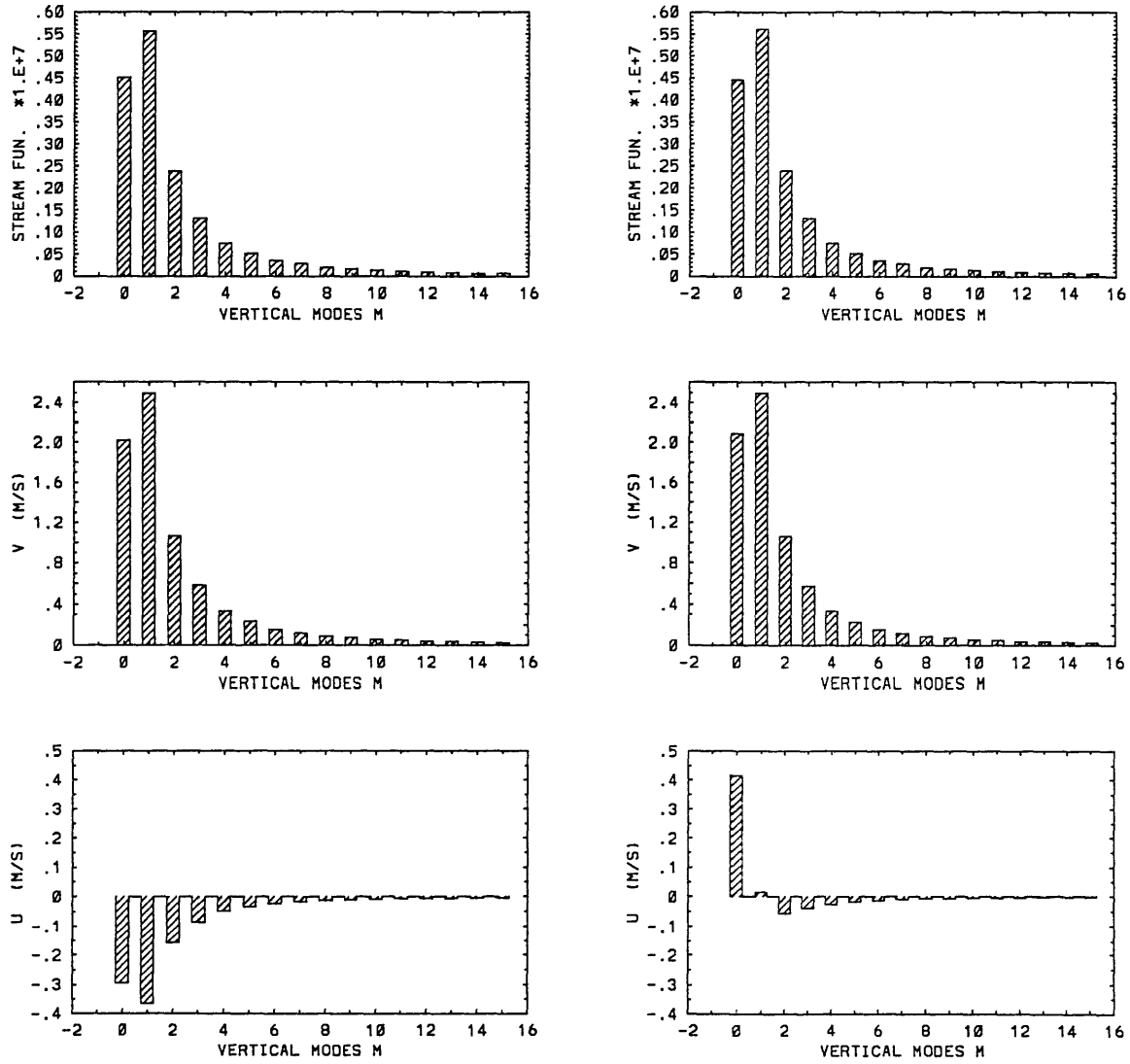


Figure 7: As in Figure 5 but for  $\bar{u} = -15.m/s$

From the upper two panels in all Fig.3-Fig.7 we found that for both the propagating and trapped waves the initialized  $\psi'$  and the initialized  $v'$  are pretty similar to the original ones in terms of their amplitude and phase/or sign. This means that the projection of  $\psi'$  and  $v'$  into gravity wave is much smaller than that into Rossby wave.

However, the lowest panels in Fig.3-Fig.7. show that the initialized  $u'$  is different from the original  $u'$  and the difference depends on the mean flow. In westerlies ranging from weak to strong, the amplitude of the leading mode, which has the largest amplitude among all other modes, changes less than twice after initialization except at  $\bar{u} = 10.m/s$ . At  $\bar{u} = 10.m/s$  the amplitude of mode zero increases about 3 times after initialization. However, the phase or the sign of each mode remains unchanged in westerlies. On the contrary, the most pronounced feature in easterly mean flows is that the sign of the first several leading modes is reversed. Moreover, in Fig.6 and Fig.7 it is found that the relative importance of the first two modes ( $m=0,1$ ) is changed. The first mode ( $m=0$ ), which is originally comparable in size to the second mode ( $m=1$ ), becomes much larger than the second one after initialization. In addition, the amplitude of the first mode increases about 5 times in  $\bar{u} = -5.m/s$ .

### 5.3 Time behavior

We plot the time behavior of the noninitialized and the initialized field  $\psi'$  within 20 days after day 0 against different mean zonal flows. First we show

in Fig.8(a)-(e) the behavior of the vertical structure of the streamfunction  $\psi'$  fixed at point ( $0^{\circ}E, 45^{\circ}N$ ). As reference we also plot the vertical structure of the initial stationary wave (day 0) and the model stationary wave in the same picture. It is found that in westerlies ranging from weak to strong the behaviors of the noninitialized and initialized fields are qualitatively similar. However, in easterlies about at day 10 the vertical structure of the initialized field begins apart from that of the noninitialized field. As time increases the initialized field behaves more and more differently from the noninitialized one. This feature can be more captured in the case of  $\bar{u} = -15.m/s$ .

Moreover, we plot in Fig.9(a)-(e) the contour of the noninitialized and initialized  $\psi'$  at 5 Km within 20 days after day 0 against different mean flows. It is found that in westerlies ranging from weak to strong the phase speed as well as the amplitude of the high and low are similar between the noninitialized and the initialized fields. In the case of  $\bar{u} = 45.m/s$  the similarity is smaller compared with that in  $\bar{u} = 10.m/s$  and  $\bar{u} = 25.m/s$ . However, in easterlies it is noticed that at day 5 the initialized field begins to oscillate in place with time compared with the noninitialized field especially in its southern part. And then the oscillation becomes more and more pronounced as time increases.

In addition, we noticed in Fig.8 and Fig.9 that in westerlies neither of the noninitialized and the initialized fields behaves like the original stationary waves. However, in easterlies, the time behavior of the noninitialized fields is near stationary. We will discuss this later.

$$\bar{u} = 10.m/s$$

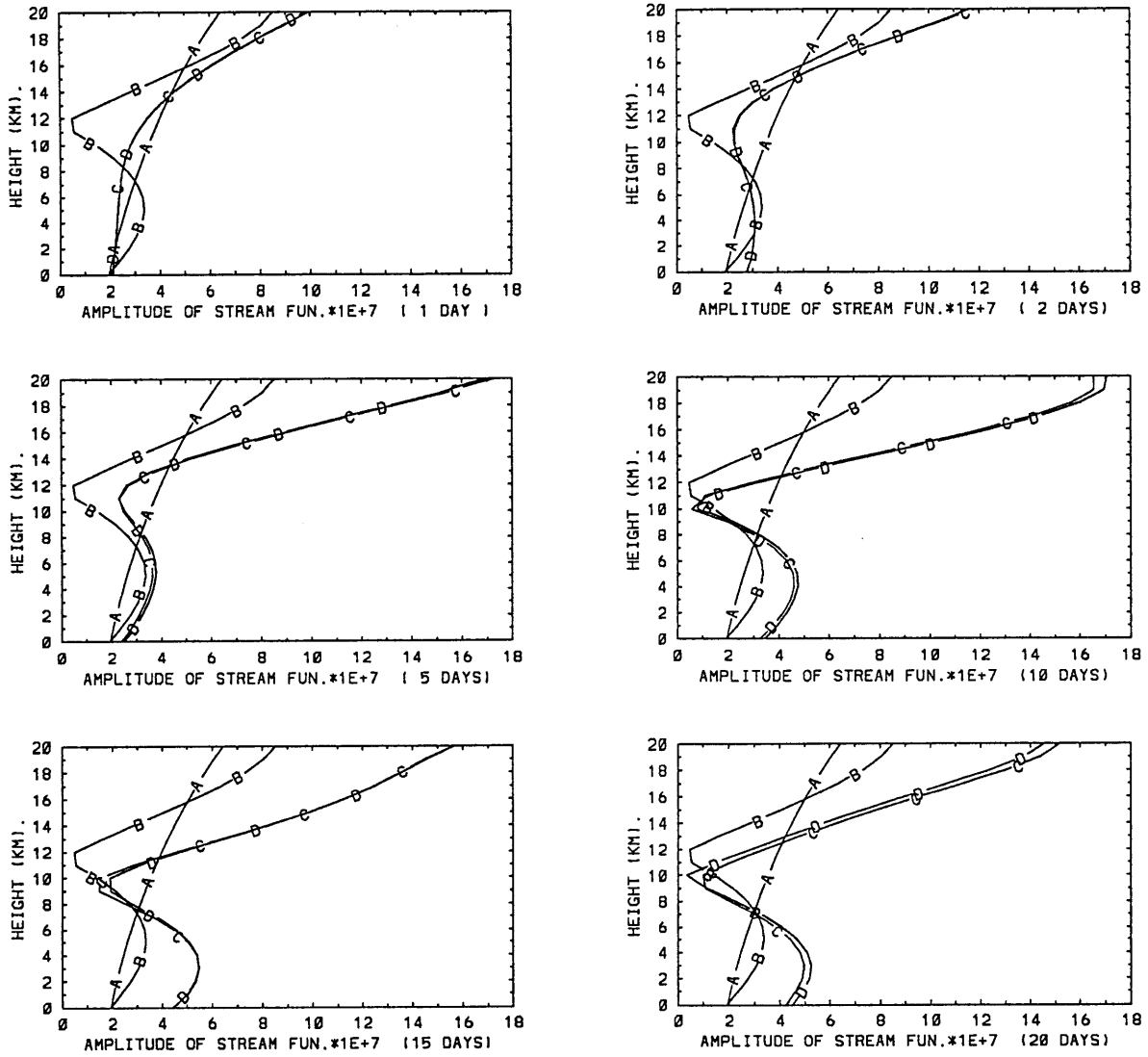


Figure 8(a): The time behavior of the vertical structure of streamfunction  $\psi'$  in  $m^2/s * 10^7$  from day 1 to day 20 for  $\bar{u} = 10.m/s$ . A: the initial stationary wave (day 0), B: the model stationary wave, C: the behavior of the noninitialized field, D: the behavior of the initialized field.

$$\bar{u} = 25.m/s$$

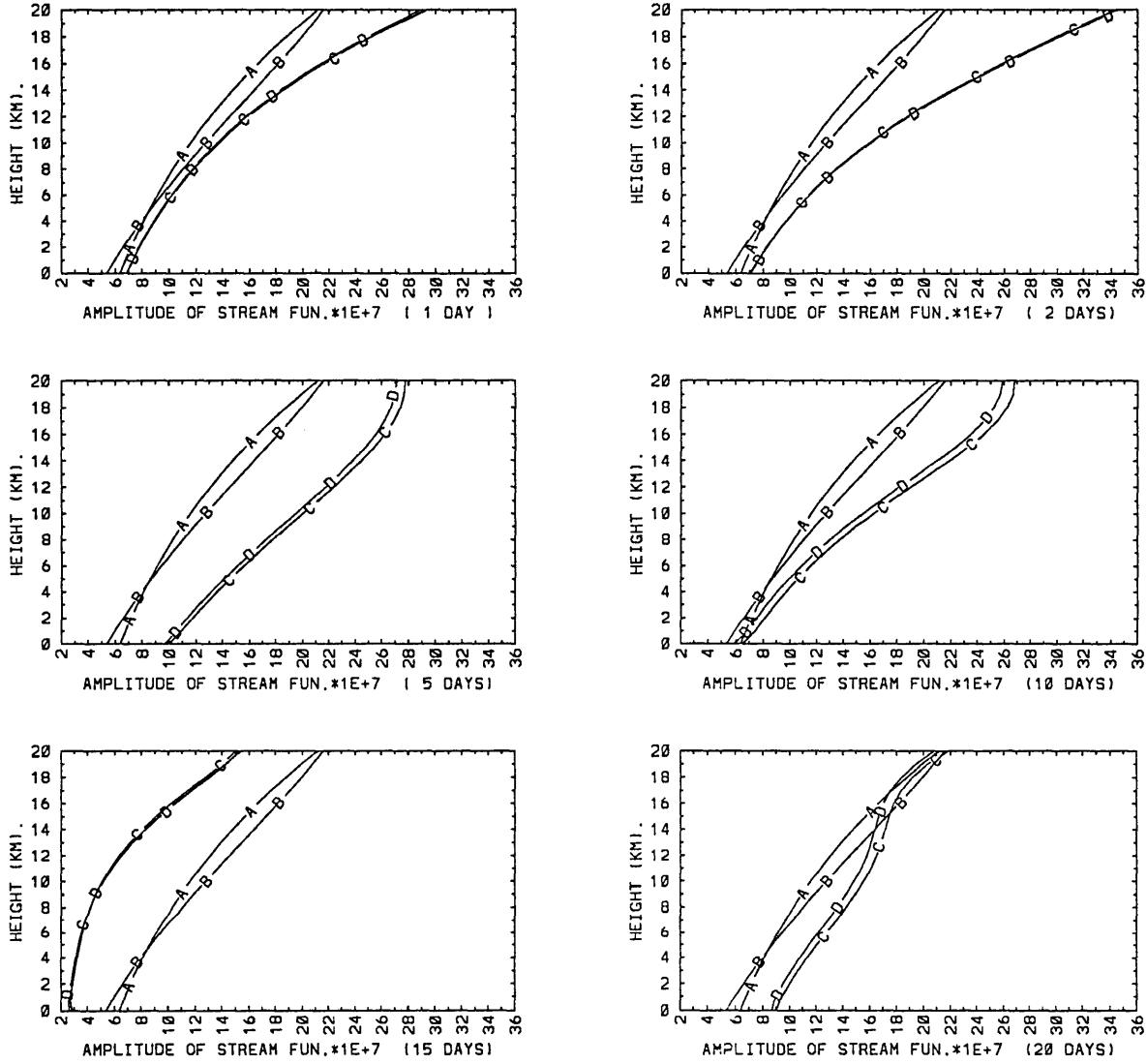


Figure 8(b): As in Figure 8(a) but for  $\bar{u} = 25.m/s$

$$\bar{u} = 45.m/s$$

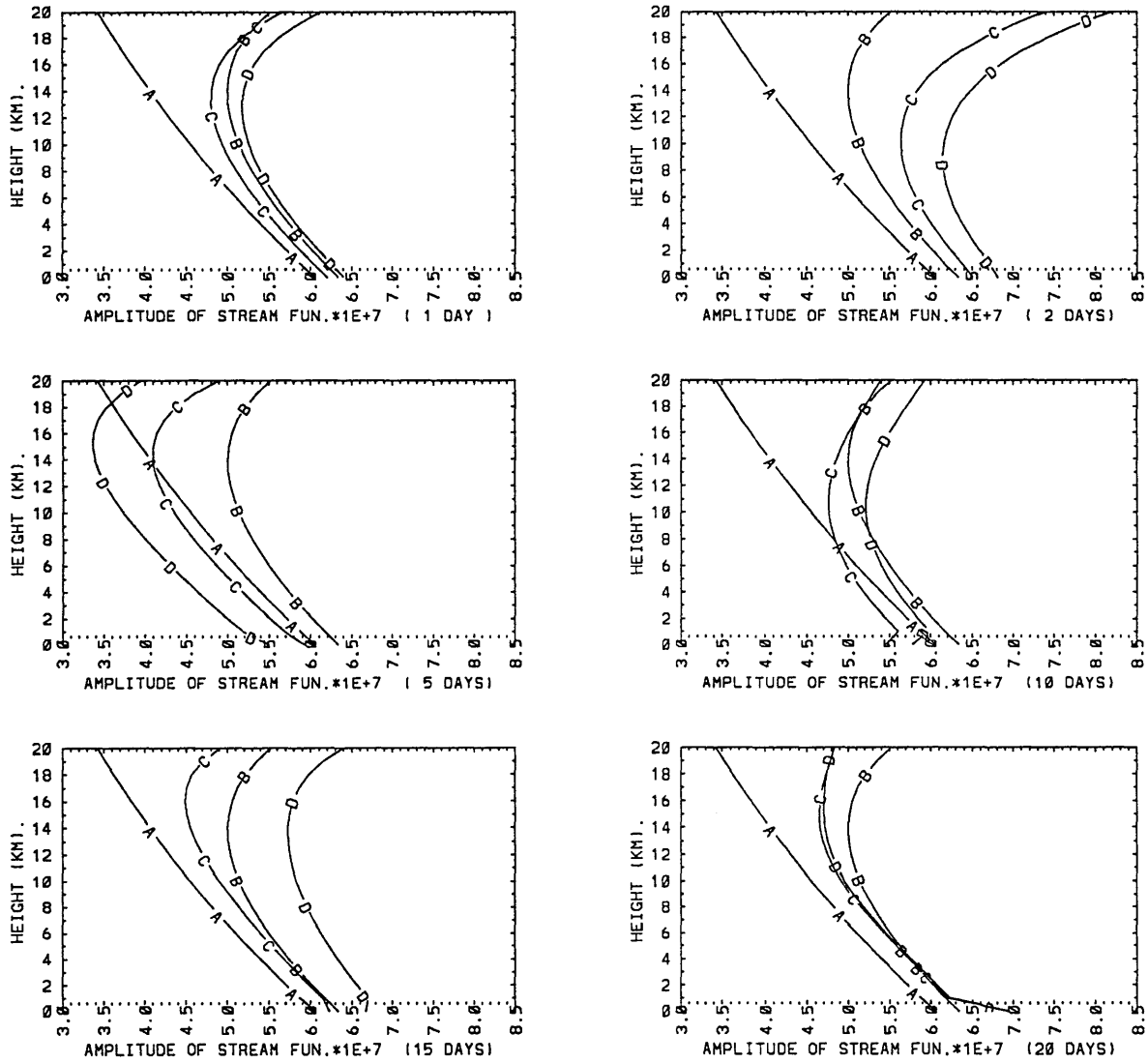


Figure 8(c): As in Figure 8(a) but for  $\bar{u} = 45.m/s$ .



$$\bar{u} = -5.m/s$$

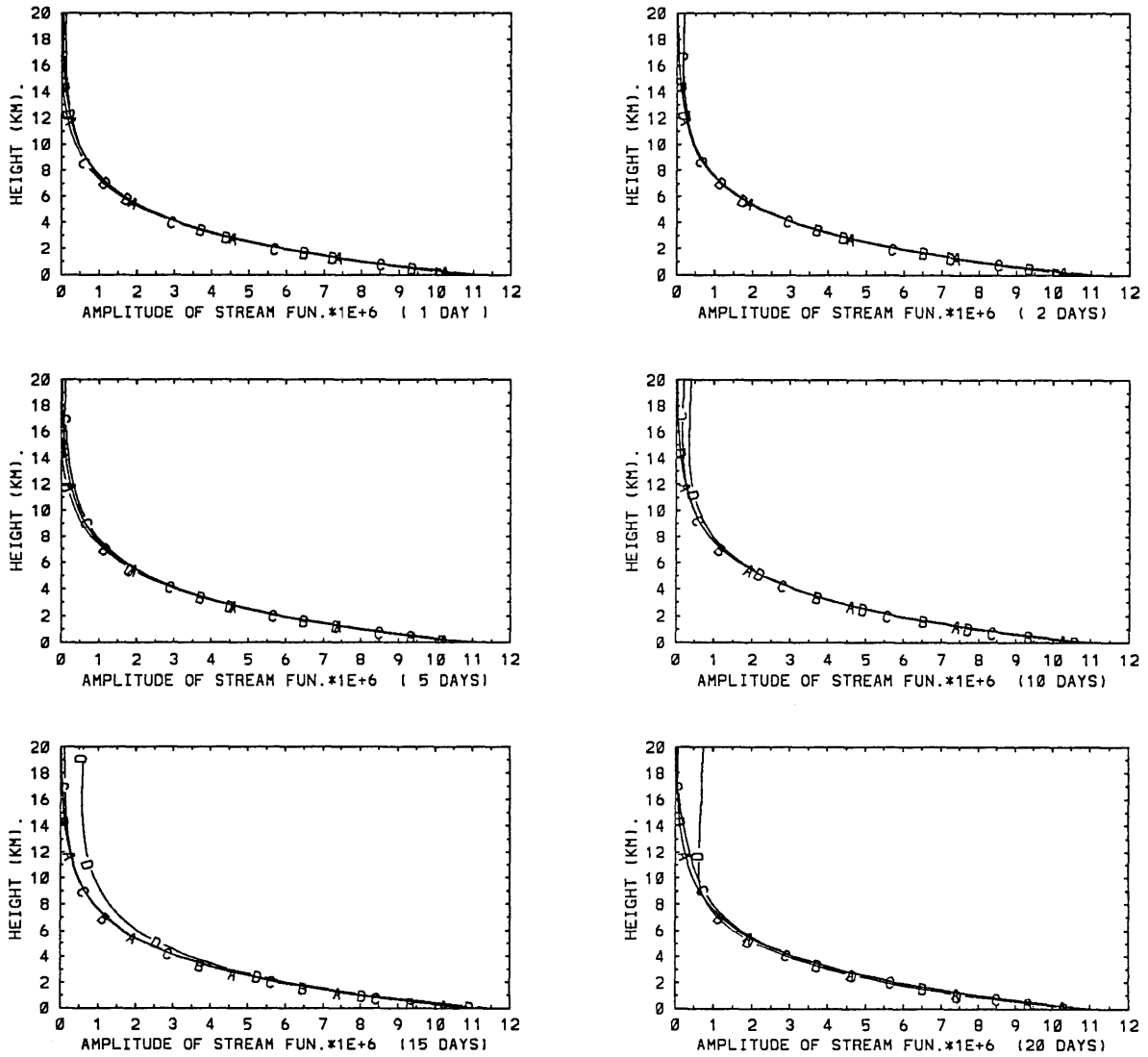


Figure 8(d): As in Figure 8(a) but for  $\bar{u} = -5.m/s$  and the unit is  $m^2/s * 10^6$ .

$$\bar{u} = -15.m/s$$

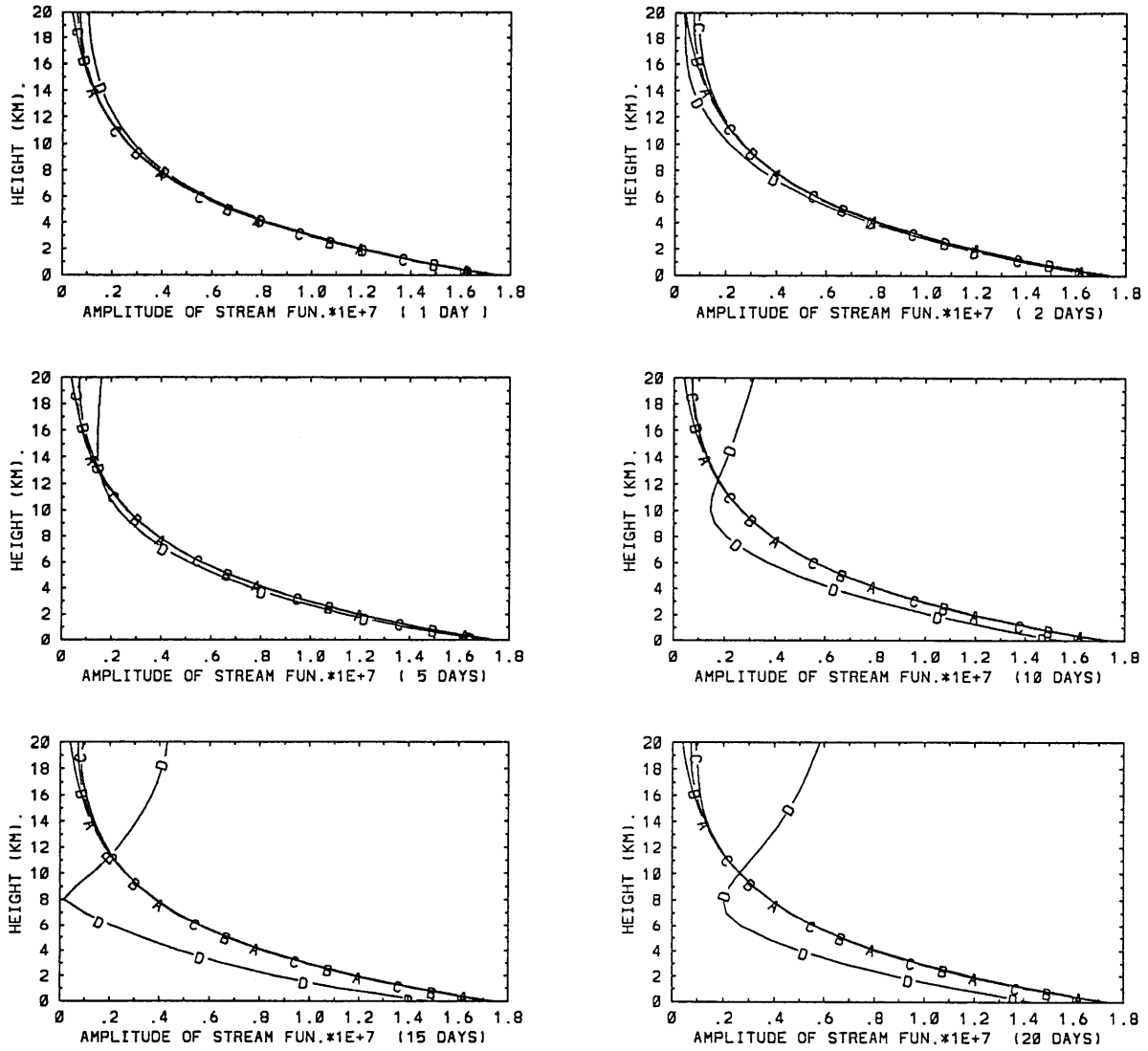


Figure 8(e): As in Figure 8(a) but for  $\bar{u} = -15.m/s$ .

$$\bar{u} = 10.m/s$$

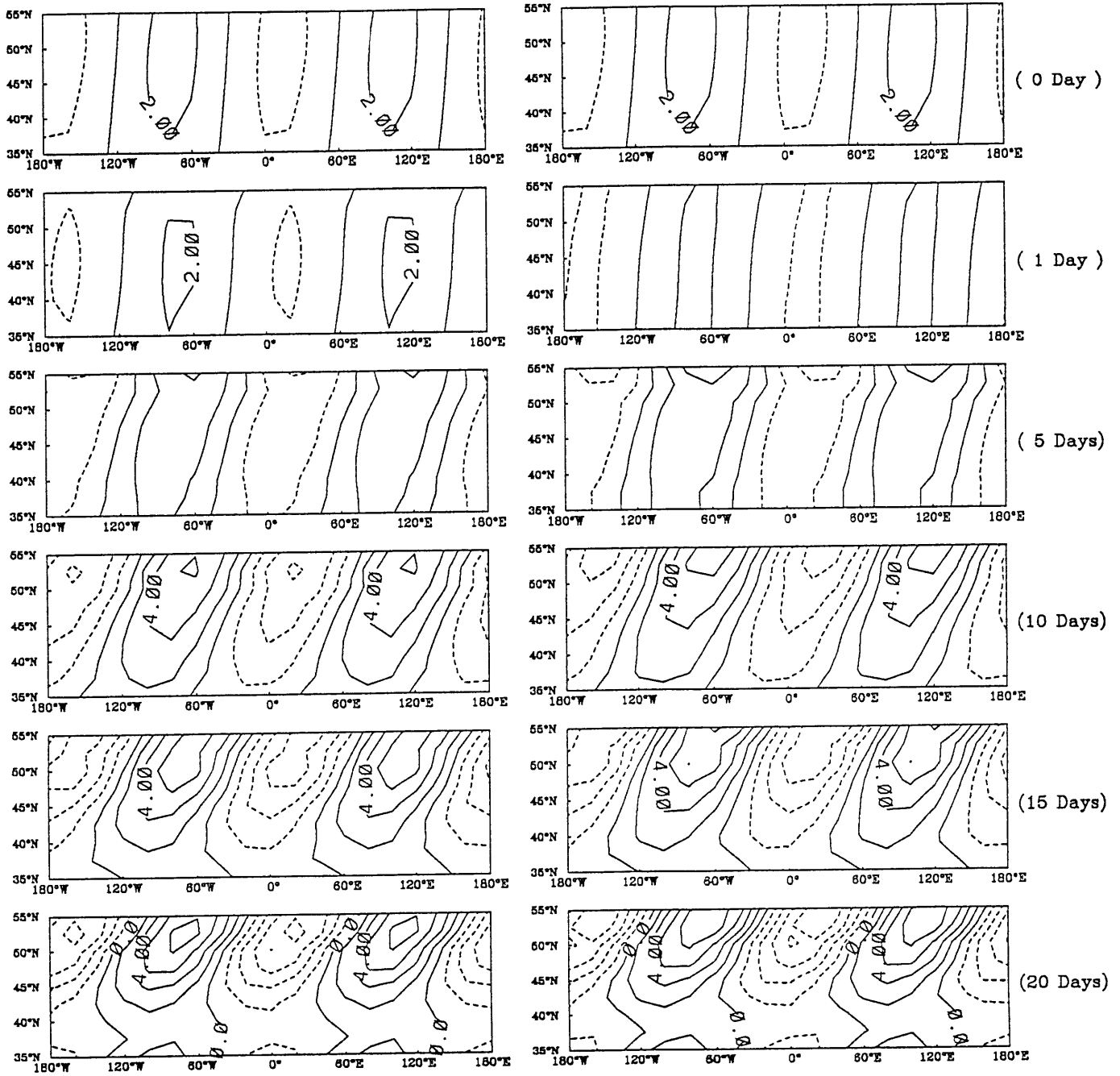


Figure 9(a): The time evolution of streamfunction at 5 Km from day 0 to day 20 for  $\bar{u} = 10.m/s$ . The contour interval is  $2.m^2/s * 10^7$  and negative contours are dashed. Left: the noninitialized field, Right: the initialized field.

$$\bar{u} = 25.m/s$$

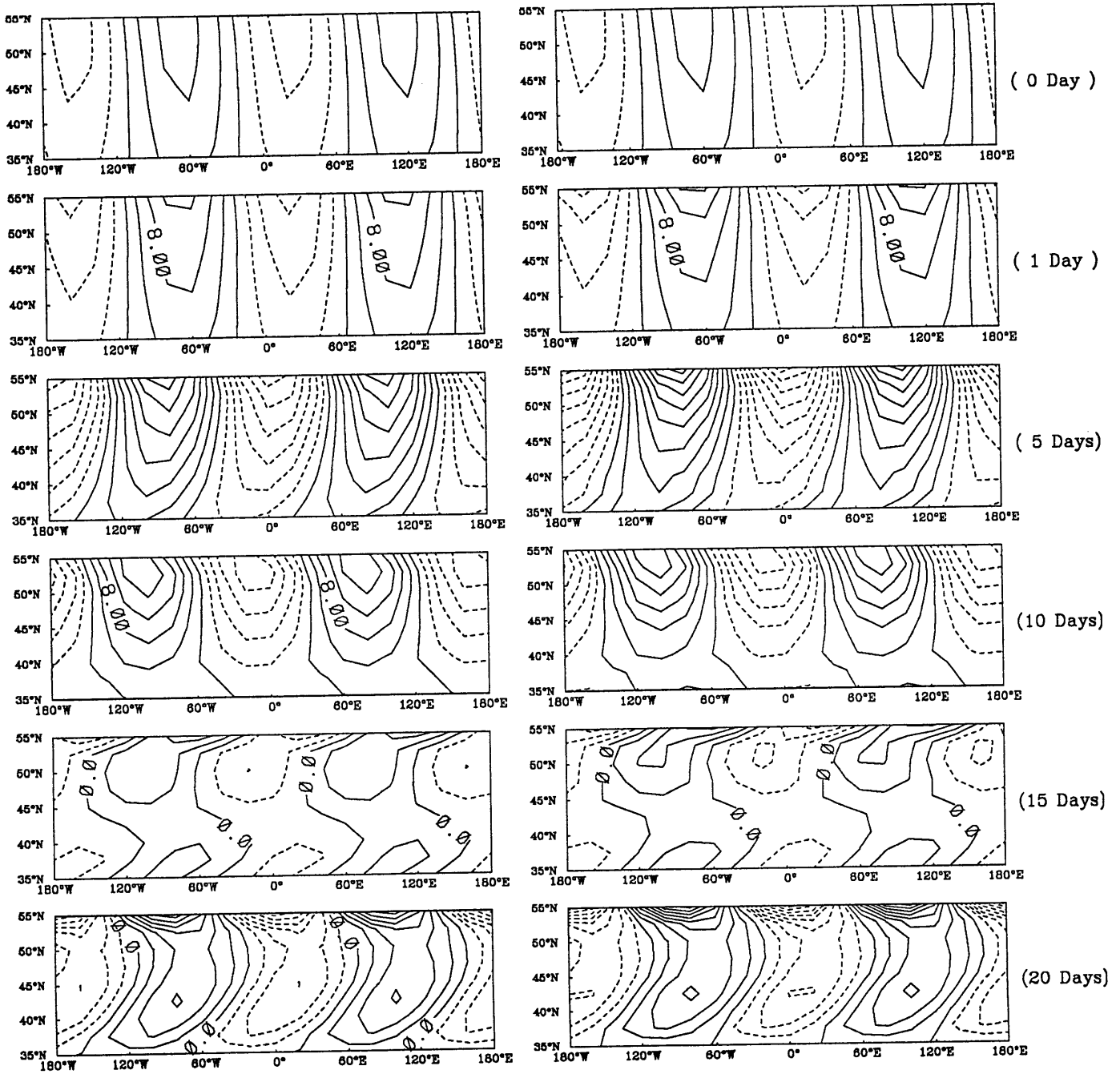


Figure 9(b): As in Figure 9(a) except that  $\bar{u} = 25.m/s$  and the contour interval is  $4.m^2/s * 10^7$ .

$$\bar{u} = 45.m/s$$

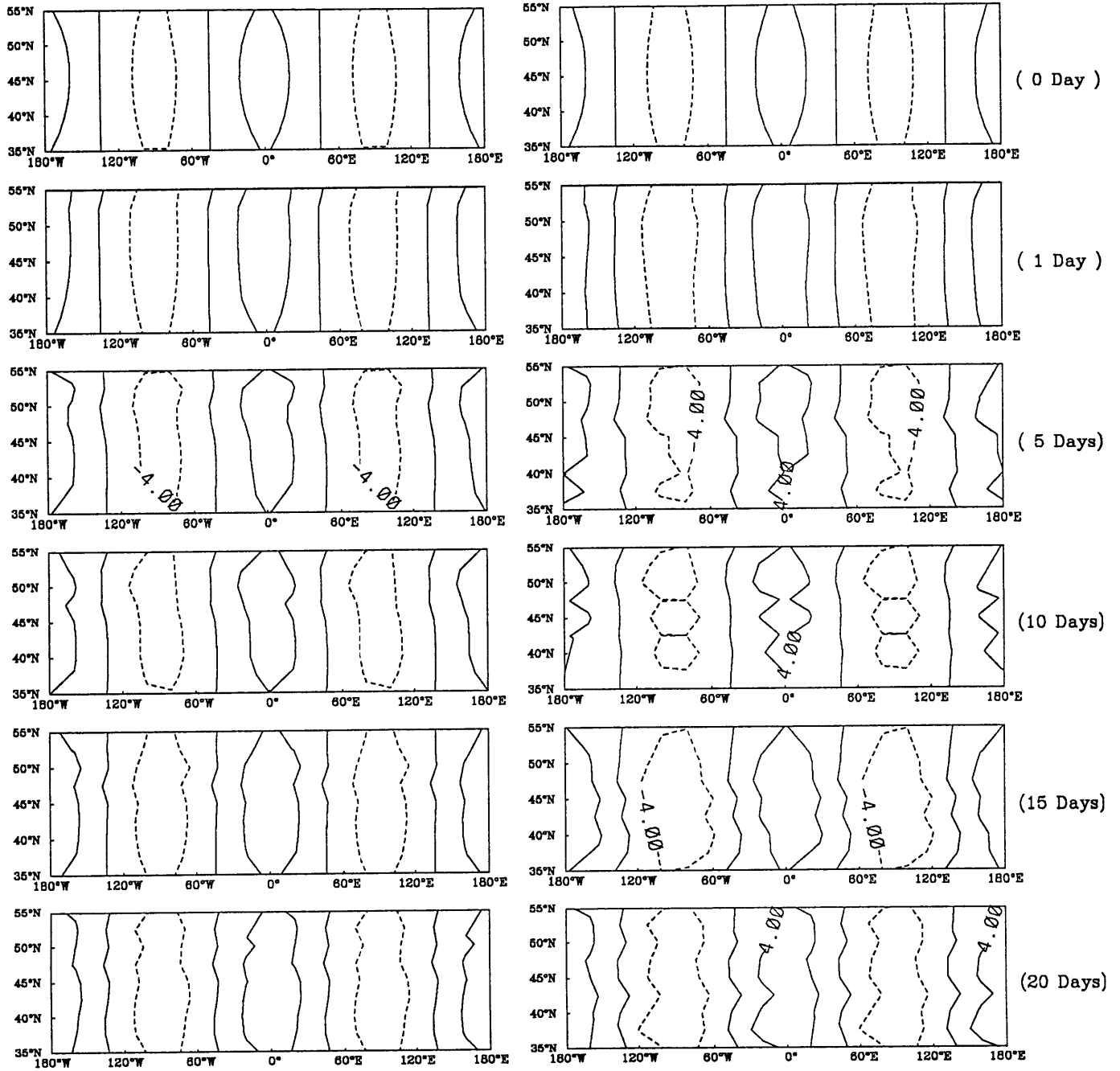


Figure 9(c): As in Figure 9(a) except that  $\bar{u} = 45.m/s$  and the contour interval is  $4.m^2/s * 10^7$ .

$$\bar{u} = -5.m/s$$

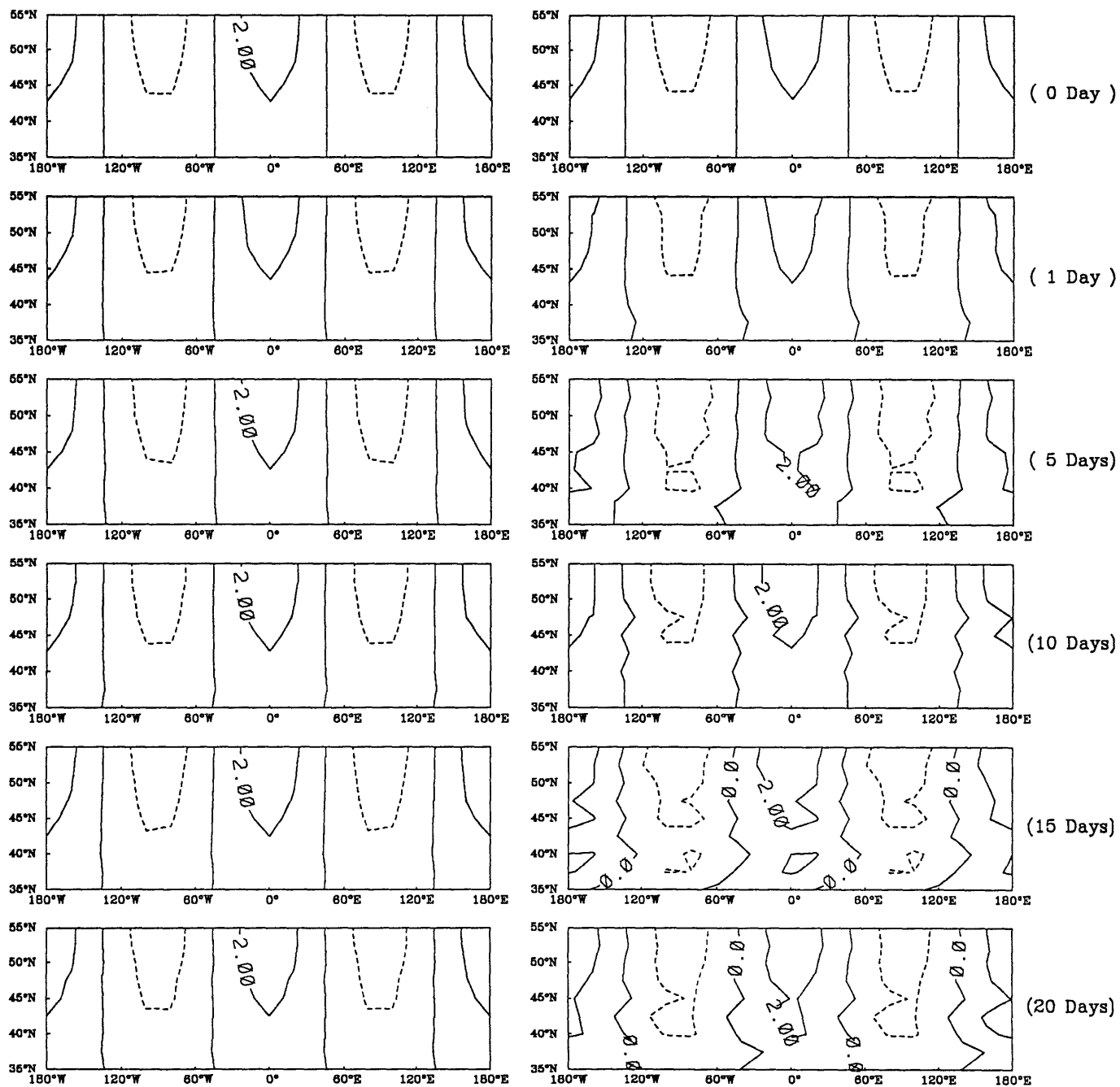


Figure 9(d): As in Figure 9(a) except that  $\bar{u} = -5.m/s$  and the contour interval is  $2.m^2/s * 10^6$ .

$$\bar{u} = -15.m/s$$

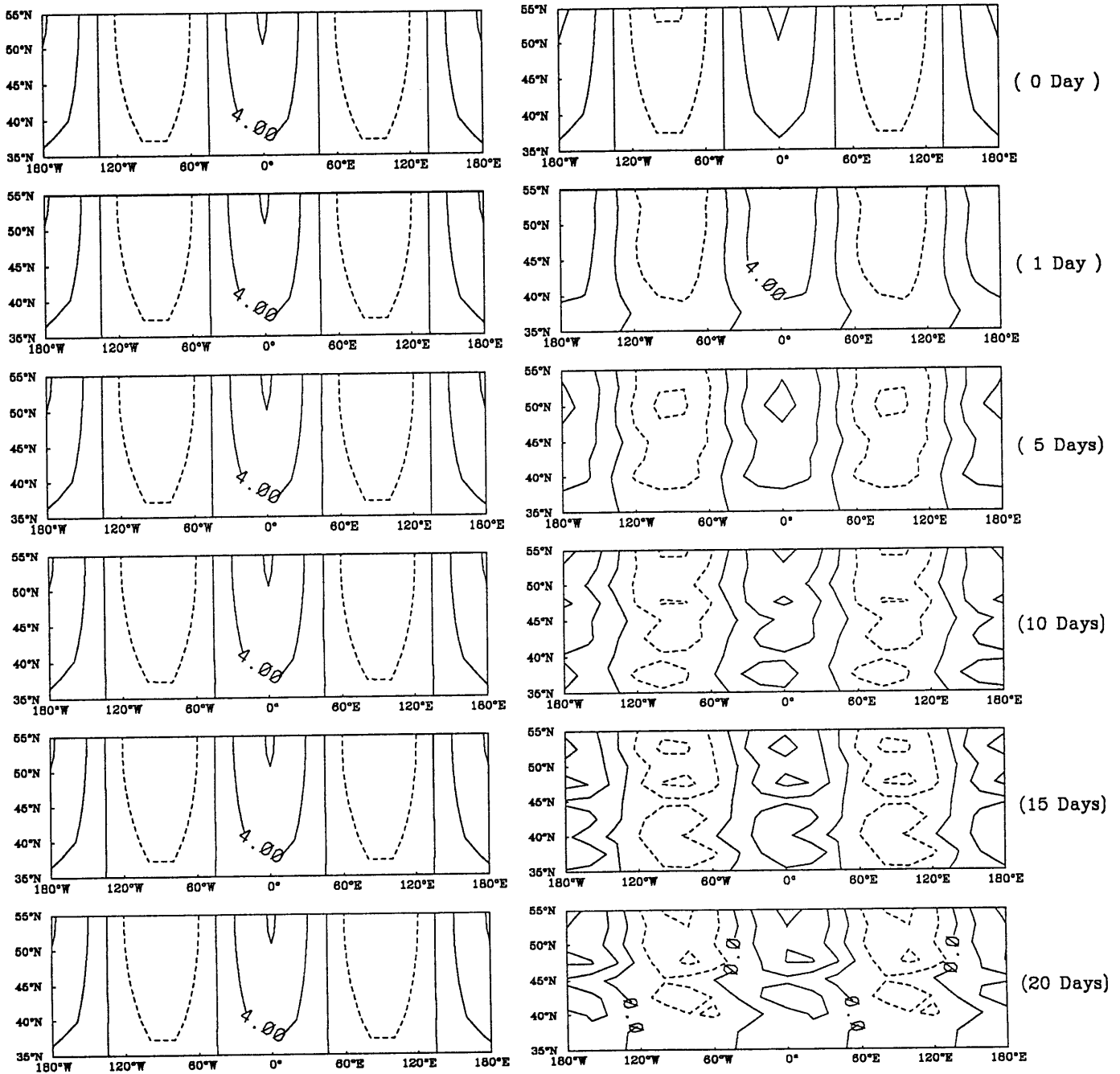


Figure 9(e): As in Figure 9(a) except that  $\bar{u} = -15.m/s$  and the contour interval is  $4.m^2/s * 10^6$ .

## 6 Discussion

### 6.1 The effect of model lid on initialization

In all of our experiments, we impose an artificial top in the model. We found that the behaviors of the initialized and noninitialized fields are similar in westerlies and different in easterlies respectively. Thus, we expect that the initialization is insensitive to the existence of model top. In order to verify this, we increased the model top to 30Km for the cases of  $\bar{u} = 10.m/s$  and  $\bar{u} = -15.m/s$  as comparison with the model top at 20Km.

Fig.10(a) and Fig.10(b) show the behavior of the vertical structure of streamfunction at ( $0^{\circ}E, 45^{\circ}N$ ) and the contour of the streamfunction at 5Km respectively for mean flow of  $\bar{u} = 10.m/s$  when the model top is at 30Km. It is found that the vertical structures for the noninitialized and the initialized fields are pretty similar within 20 days. Moreover, the contour of the initialized field looks like the noninitialized one. Thus the behavior of the initialized field is generally in agreement with that of the noninitialized one when the model top is placed at 30Km.

Fig.11(a) and Fig.11(b) show the behaviors of the noninitialized and the initialized fields for the mean flow of  $\bar{u} = -15.m/s$  when the model top is at 30Km. It is found that in easterly the initialized field begins apart from the noninitialized one at day 5. As time increases the initialized field behaves more differently from the noninitialized one.



$$\bar{u} = 10.m/s$$

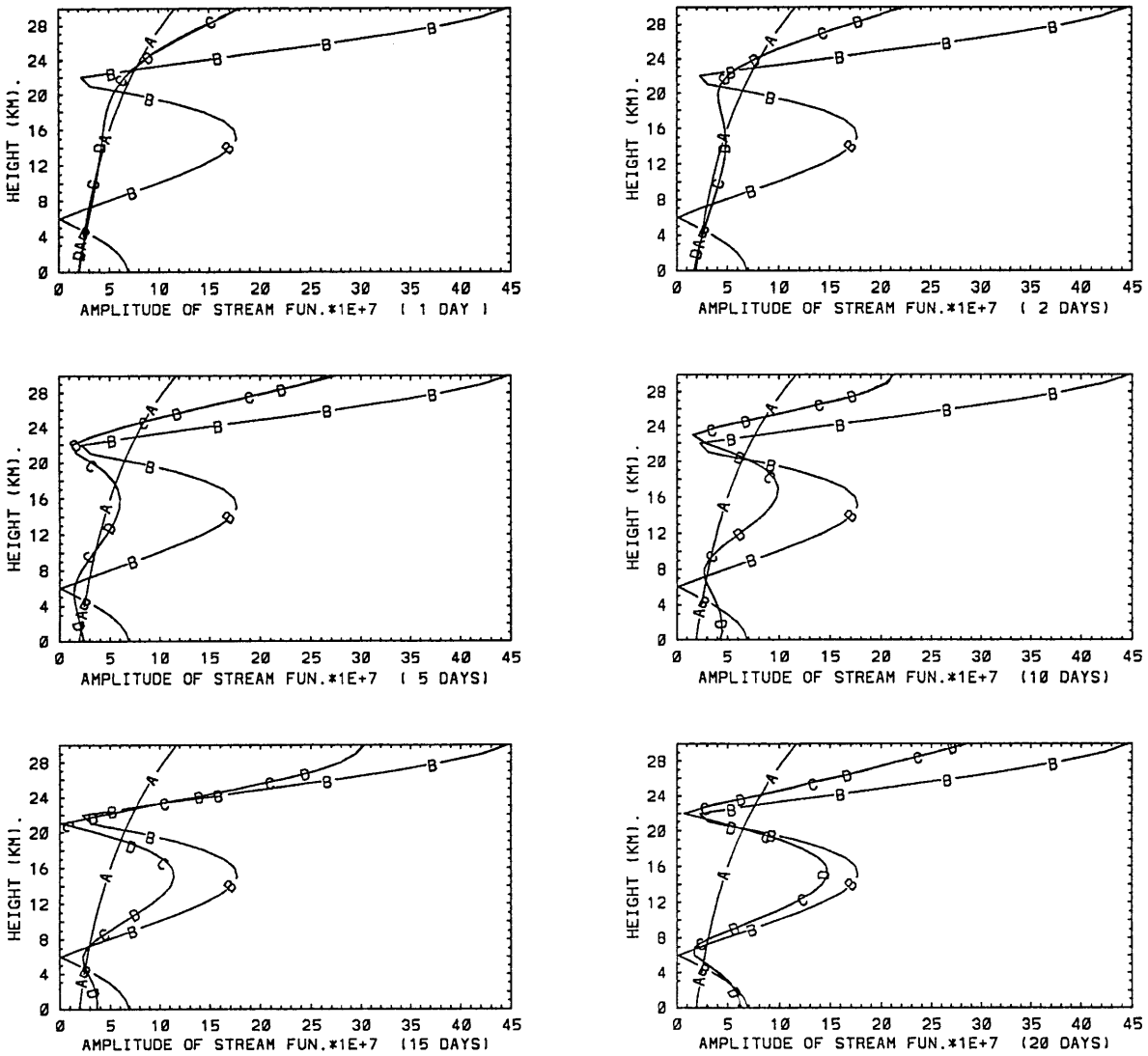


Figure 10(a): The time behavior of the vertical structure of stream-function in  $m^2/s * 10^7$  from day 1 to day 20 for  $\bar{u} = 10.m/s$ . The model top is at 30Km. A: the initial stationary wave(day 0), B: the model stationary wave, C: the behavior of the noninitialized field, D: the behavior of the initialized field.

$$\bar{u} = 10.m/s$$

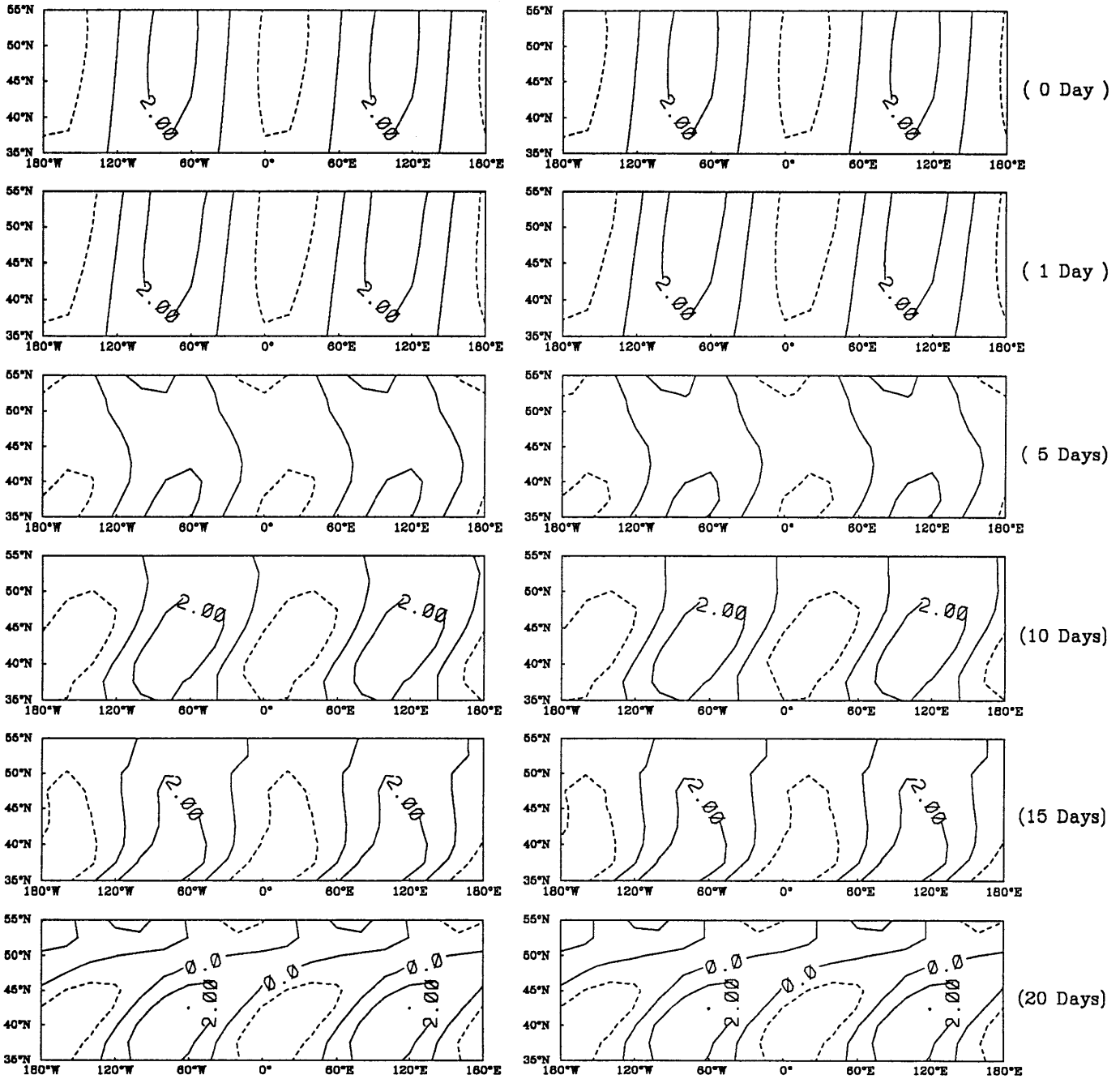


Figure 10(b): The time evolution of streamfunction at 5Km from day 0 to day 20 for  $\bar{u} = 10.m/s$ . The model top is at 30Km. The contour interval is  $2.m^2/s * 10^7$  and negative contours are dashed.

$$\bar{u} = -15.m/s$$

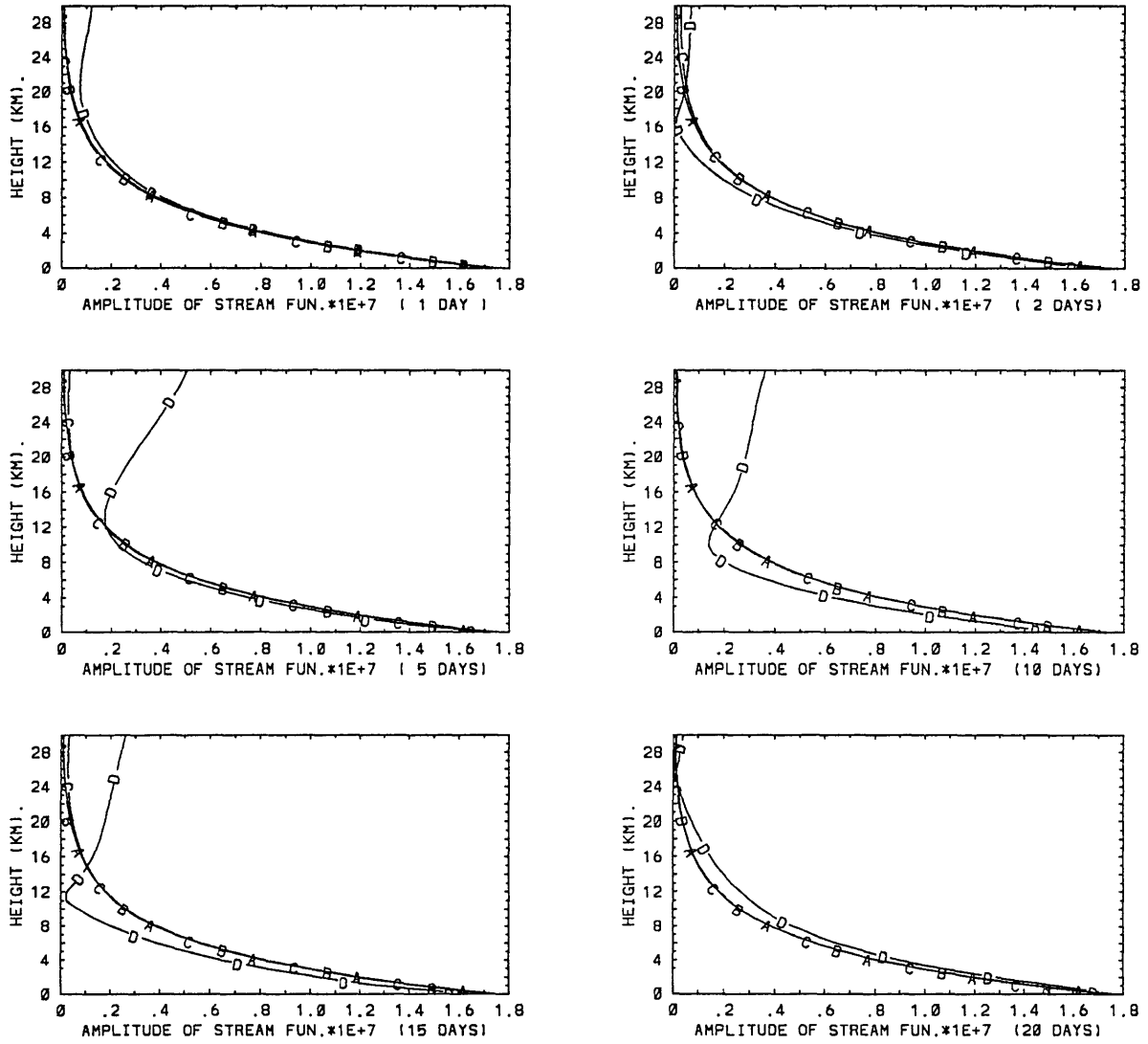


Figure 11(a): As in Figure 10(a) but for  $\bar{u} = -15.m/s$ .

$$\bar{u} = -15.m/s$$

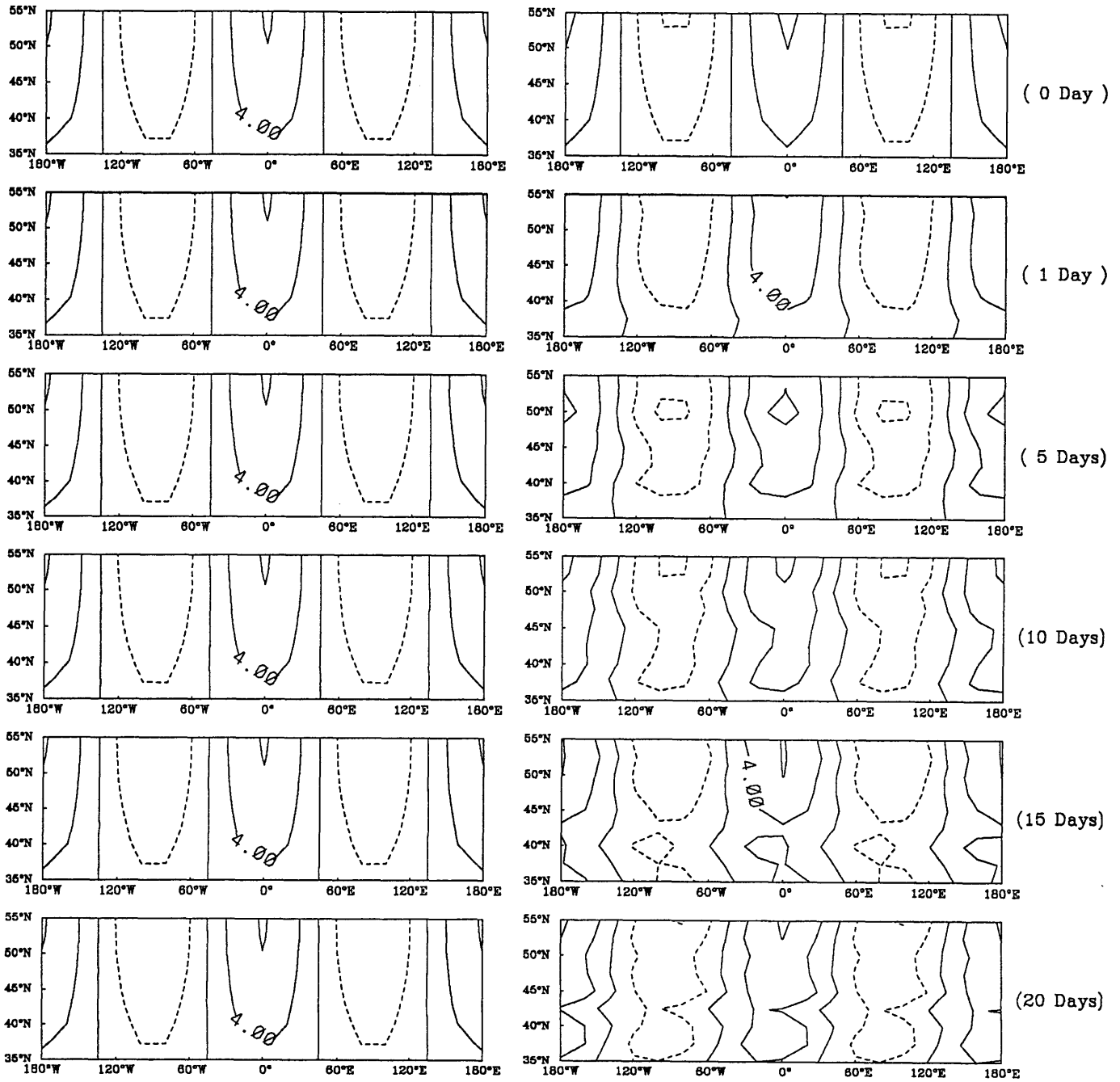


Figure 11(b): As in Figure 10(b) except that  $\bar{u} = -15.m/s$  and the contour interval is  $4.m^2/s * 10^6$ .

Therefore, the results from the study of model top at 30Km are in agreement with those from the study of model top at 20Km. This confirms that the existence of model lid does not affect initialization.

## 6.2 The sensitivity of initialization to mean zonal flows

We have found before that the time behaviors of the initialized fields look like those of the noninitialized ones in westerlies ranging from weak to strong. However, this does not hold in easterlies. In order to investigate why the time behavior of the initialized field depends on the mean flow, we recall the results from the normal mode initialization.

We have seen before that in westerlies in spite of small changes of the size of  $u'$ , the phases or the signs of  $u'$  remain unchanged. However, in easterlies the first two leading modes ( $m=0,1$ ) are heavily affected by the loss of gravity part in terms of the sign, the relative importance and the amplitude. Since the initial field is stationary wave, namely  $c = 0$ , according to wave phase speed:

$$c = \bar{U} - \frac{\beta}{k^2 + l^2 + \frac{f_0^2}{gh}} \quad (90)$$

where  $h$  is the equivalent depth, in the presence of westerly mean flow Rossby wave propagates westward, while in the presence of easterly mean flow Rossby wave propagates eastward. However, eastward Rossby wave is not the eigenmode of the 3X3 eigenmatrix in equation(64), and therefore the initial stationary wave can not be corrected projected into the eigen system.

Thus, we conclude that the change of the mode structure after initialization is sensitive to mean flow and the change is crucial to the future behavior of the stationary wave. However, questions still remain about the relevance of initialization to more realistic mean flows such as vertical wind shear.

### 6.3 The role of vertical wind shear

In order to investigate how the behaviors of the initialized and the non-initialized fields are affected by vertical wind shear, we did some simple experiments as comparison. The wind shears are chosen as one case of all westerlies from surface to top and two cases of weaker and stronger easterlies near surface respectively and westerlies above. These are:

- (a)  $\bar{u}(z)$  is from 5.m/s at surface to 40.m/s at top.
- (b)  $\bar{u}(z)$  is from -5.m/s at surface to 25.m/s at top.
- (c)  $\bar{u}(z)$  is from -15.m/s at surface to 25.m/s at top.

The three different  $\bar{u}(z)$  distributions are shown in Fig.12.

In the presence of vertical wind shear, the initial field is still the solution to equation(24) or equation(28) as we used before, but solved numerically. The radiation condition in model top is assumed as:

$$\frac{d\Psi}{dz} = -i\gamma\Psi \quad (91)$$

where  $\gamma$  is the same as in equation(32), and  $Im(\gamma) < 0$  is required. The initial field is then projected into normal modes by using discrete Fourier transform.

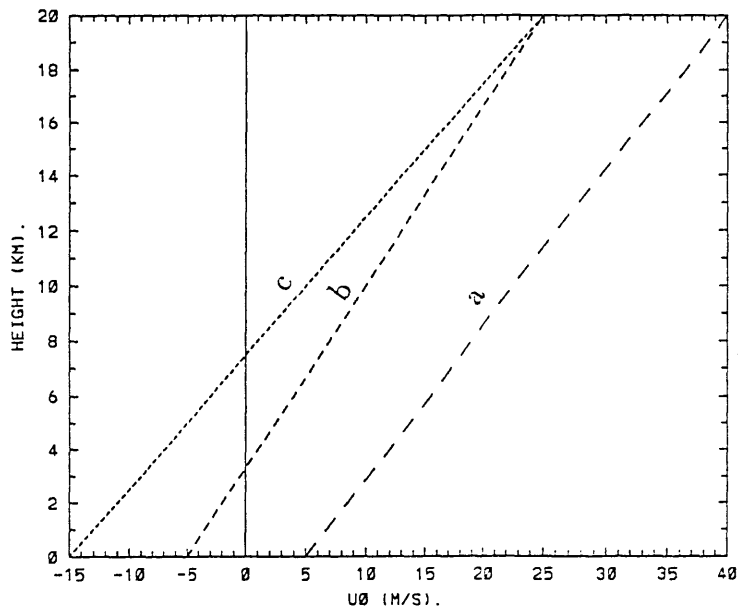


Figure 12: The vertical distribution of wind shear. a) in long dashed line:  $\bar{u}$  from  $5.m/s$  to  $40.m/s$ , b) in short dashed line:  $\bar{u}$  from  $-5.m/s$  to  $25.m/s$ , c) in dotted line:  $\bar{u}$  from  $-15.m/s$  to  $25.m/s$ . The solid line is zero wind line.

The results of the time integration of the noninitialized and the initialized fields are plotted in Fig.13 and Fig.14. Fig.13(a)-(c) shows the behaviors of the vertical structure of streamfunction at  $(0^{\circ}E, 45^{\circ}N)$  for the cases of

shear(a)-(c) respectively. Again as reference the initial stationary wave with radiation condition and the model stationary wave with lid are plotted in the same picture. In case(a) the initial stationary wave is propagating from surface to about 11Km then turns trapped on top, while in both case(b) and case(c) the initial stationary waves are first trapped from surface and then propagating upward with the latter trapped less heavily.

Comparison from Fig.13(a)-(c) shows that in all three cases the behaviors of the initialized and the noninitialized fields generally bear resemblance. However, it is noticed that there is some slight difference of the behaviors of the initialized and the noninitialized fields in different time scales except in case(c), where the behavior of the initialized field is pretty similar to that of the noninitialized one in all 20 days. In case(a) the initialized field is similar to the noninitialized one in the first several days, but at day 10 it differs most especially in the upper part. Finally this difference seems diminishing with time. However, in case(b) the initialized field differs most from the noninitialized one in the first several days until at day 10. After day 10 the behaviors of the initialized and the noninitialized field look much more similar than before.

Fig.14(a)-(c) shows the contour of streamfunction at 5Km for cases(a)-(c) respectively. It is found that in all three cases the behaviors of the initialized fields are pretty similar to those of the noninitialized ones not only in size and phase speed but also the fine structures of contours.



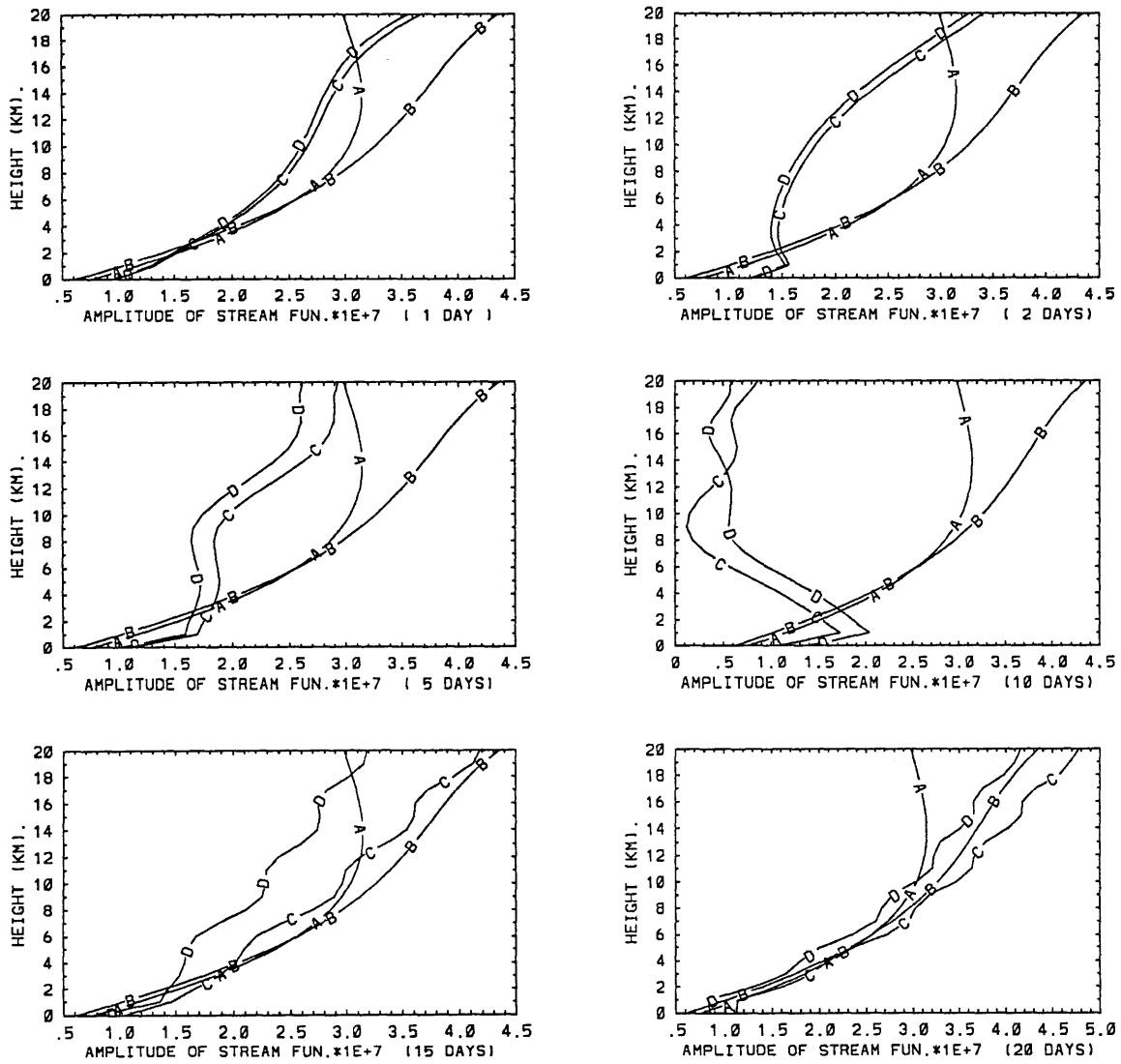


Figure 13(a): The time behavior of the vertical structure of stream-function in  $m^2/s * 10^7$  from day 1 to day 20 for shear (a). A: the initial stationary wave(day 0), B: the model stationary wave, C: the behavior of the noninitialized field, D: the behavior of the initialized field.

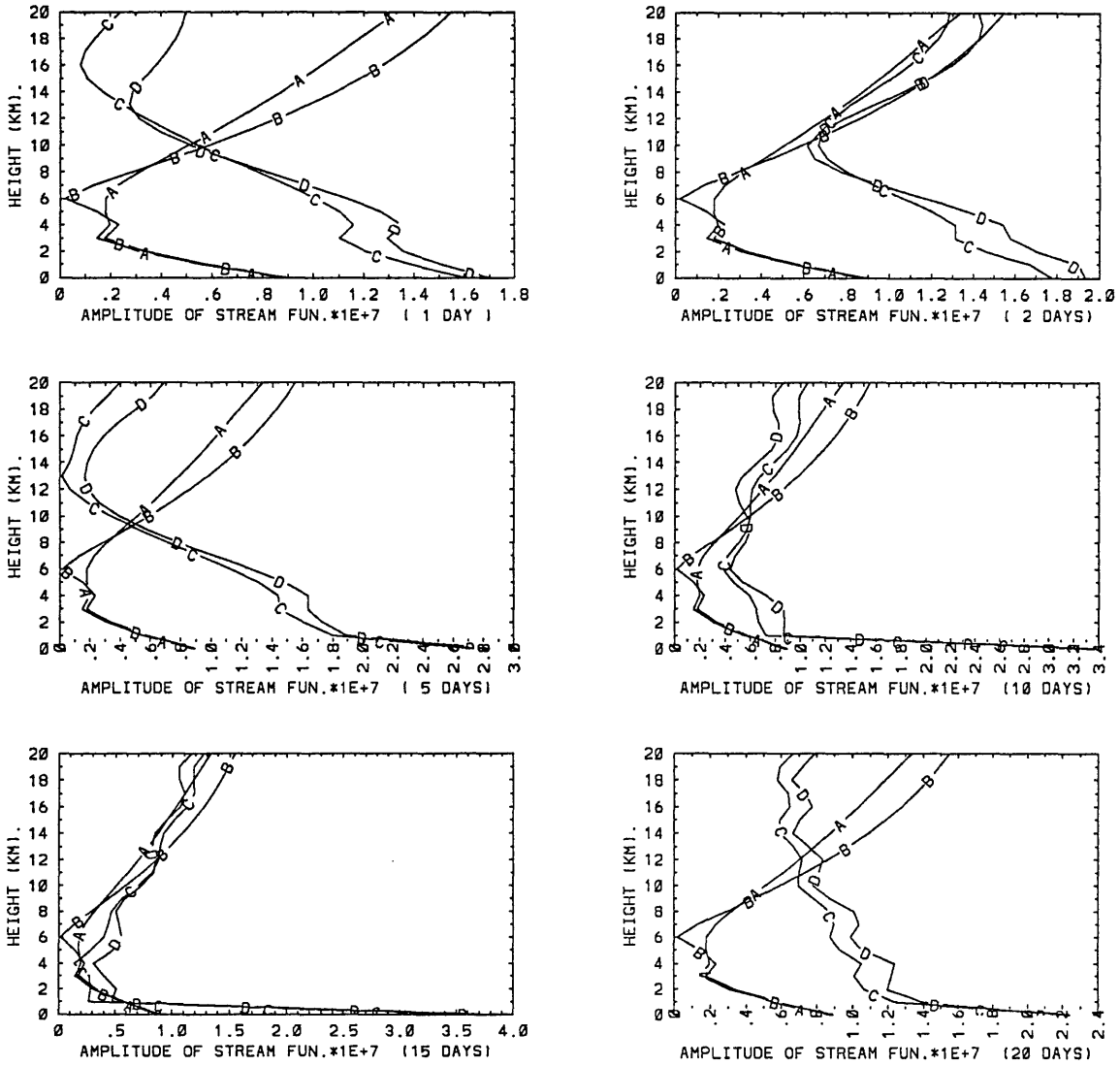


Figure 13(b): As in Figure 13(a) but for shear (b).

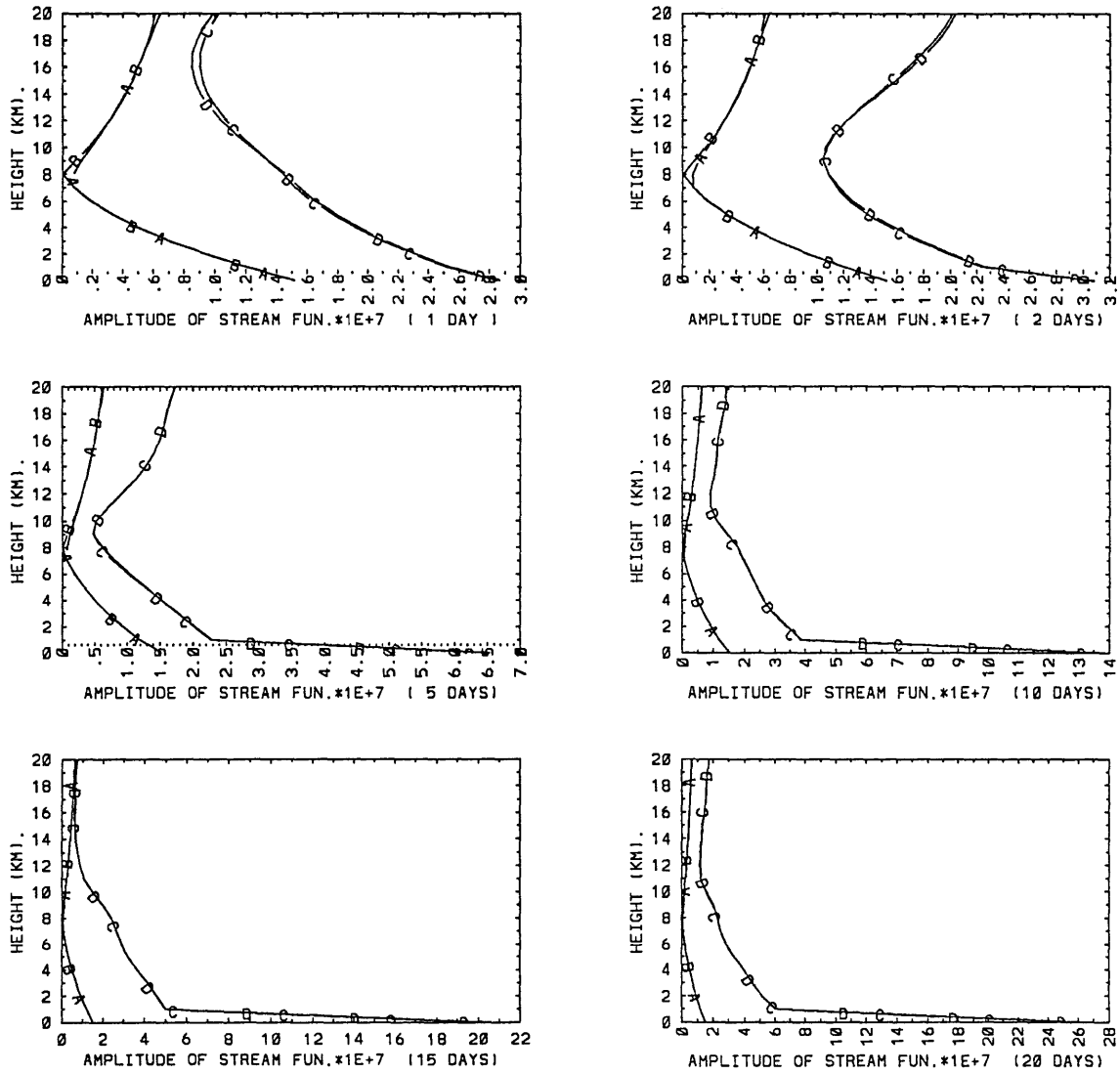


Figure 13(c): As in Figure 13(a) but for shear (c).

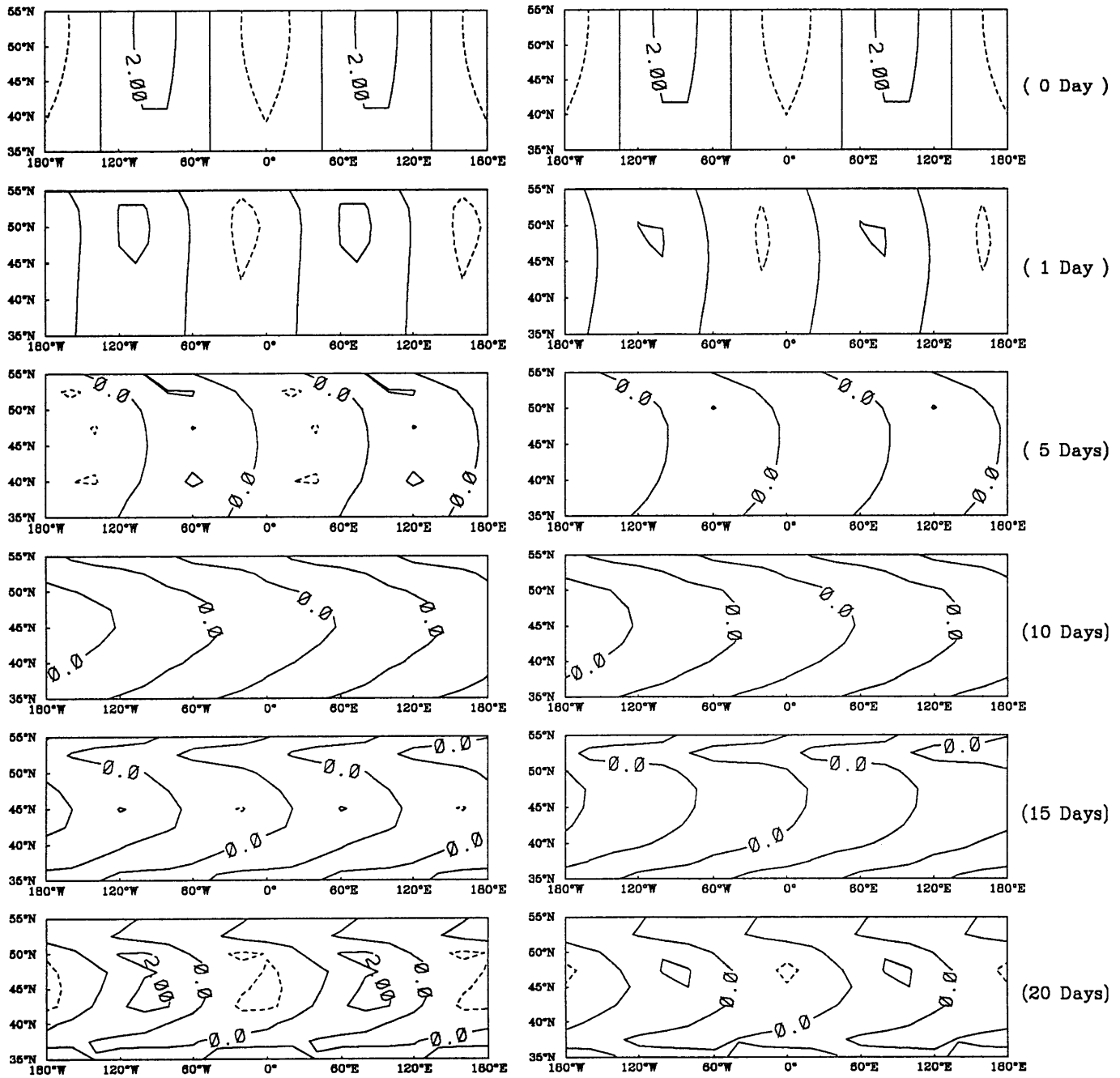


Figure 14(a): The time evolution of streamfunction at 5Km from day 0 to day 20 for shear (a). The contour interval is  $2.m^2/s * 10^7$  and the negative contours are dashed. Left: the noninitialized field, Right: the initialized field.

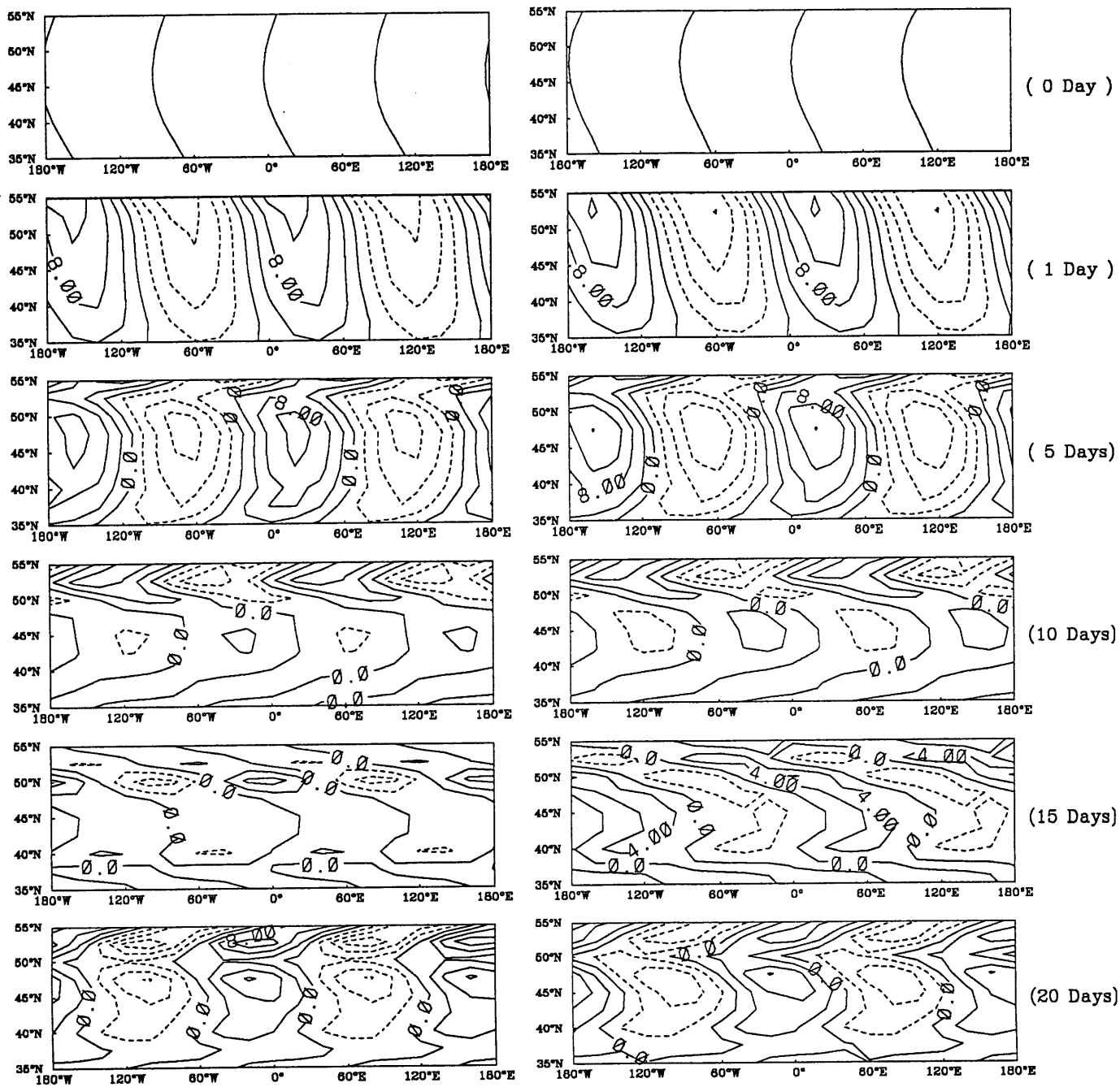


Figure 14(b): As in Figure 14(a) except for shear (b) and the contour interval is  $4.m^2/s * 10^6$ .

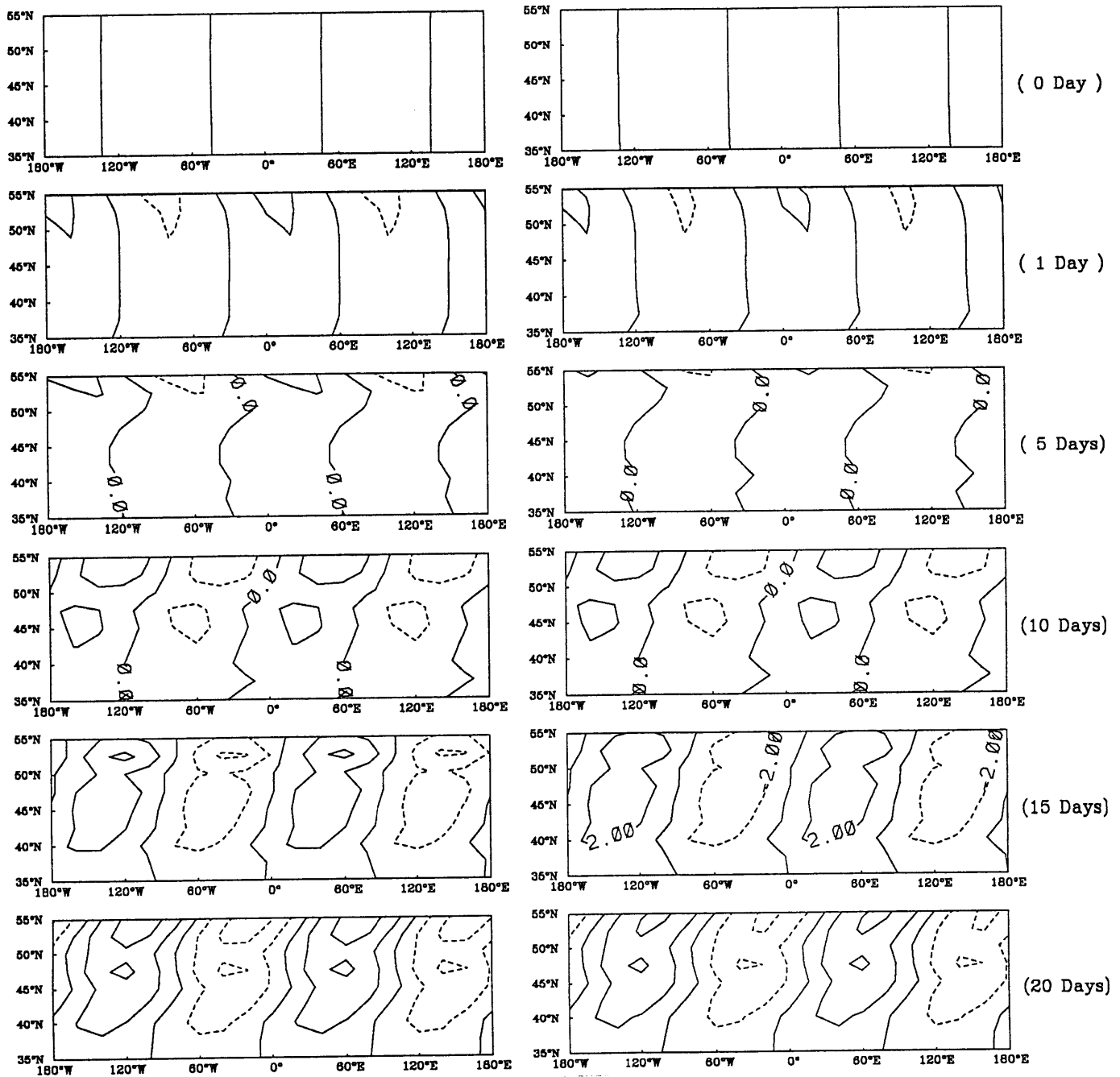


Figure 14(c): As in Figure 14(a) except for shear (c) and the contour interval is  $2.m^2/s * 10^7$ .

The above results show the similarity among all three cases. The resemblance of the time behaviors of the initialized and the noninitialized fields in both case(b) and case(c) is a little surprising and interesting, as we found before that in the presence of uniform easterlies the time behaviors of the initialized and the noninitialized fields are different. It seems that the effect of the easterlies near surface is vanishing in the presence of mean shear. It is not clear that this is because westerlies are dominant in the domain and easterlies are small. Therefore, it is necessary to further investigate the situation of mean flows with both easterlies and westerlies.

#### **6.4 The departure of the evolution of the stationary wave from its initial state**

Although we have found that initialization is not affected much by the existence of model lid, there is some other problem rising from the placement of a model lid. We noticed in Fig.8(a)-(e) and Fig.13(a)-(c) that the vertical structures of both the initialized and the noninitialized fields behave differently from those of the initial fields. As planetary stationary waves are concerned, their time solutions should not change at all in nature. However, due to the existence of model lid the difference field of the initial stationary wave and the model stationary wave travels with the phase speed of free Rossby wave. In order to see how much the time behavior of the stationary wave is different from its initial state, we calculated the change of total energy with time to estimate this difference.

The energy equations involved in our time-dependent linearized baroclinic primitive model can be derived from equations(71)-(76):

$$\frac{\partial}{\partial t} \frac{1}{2} \bar{\rho} |\vec{v}'|^2 = -\bar{u} \frac{\partial}{\partial x} \frac{1}{2} \bar{\rho} |\vec{v}'|^2 - \nabla \cdot p' \vec{v}' + p' \nabla \cdot \vec{v}' \quad (92)$$

$$\frac{\partial}{\partial t} \frac{1}{2} \frac{c_v}{c_p} \frac{p'^2}{\bar{p}} = -\bar{u} \frac{\partial}{\partial x} \frac{1}{2} \frac{c_v}{c_p} \frac{p'^2}{\bar{p}} - p' \nabla \cdot \vec{v}' - \frac{p'}{\bar{\rho}} \frac{\partial \bar{\rho} w'}{\partial z} - \frac{N^2}{g} p' w' \quad (93)$$

where  $\nabla \cdot$  denotes the divergence in x, y plane, and  $\frac{1}{2} \bar{\rho} |\vec{v}'|^2$  and  $\frac{1}{2} \frac{c_v}{c_p} \frac{p'^2}{\bar{p}}$  are defined as kinetic energy and internal energy respectively. Now integrate equations(92)-(93) over x, y, z domain:

$$\frac{\partial}{\partial t} \iiint \frac{1}{2} \bar{\rho} |\vec{v}'|^2 dx dy dz = \iiint p' \nabla \cdot \vec{v}' dx dy dz \quad (94)$$

$$\begin{aligned} \frac{\partial}{\partial t} \iiint \frac{1}{2} \frac{c_v}{c_p} \frac{p'^2}{\bar{p}} dx dy dz &= \iiint -p' \nabla \cdot \vec{v}' dx dy dz - \iiint \frac{p'}{\bar{\rho}} \frac{\partial \bar{\rho} w'}{\partial z} dx dy dz \\ &- \iiint \frac{N^2}{g} p' w' dx dy dz \end{aligned} \quad (95)$$

The advection terms  $\bar{u} \frac{\partial}{\partial x}$  in equations(92)-(93) and the  $\nabla \cdot p' \vec{v}'$  term in equation(92) drop out because of the continuity in x direction and the zero normal velocity at y boundary. Then adding equation(94) and equation(95), we get the rate of the change of total energy in whole domain:

$$\begin{aligned} \frac{\partial}{\partial t} \iiint \left( \frac{1}{2} \bar{\rho} |\vec{v}'|^2 + \frac{1}{2} \frac{c_v}{c_p} \frac{p'^2}{\bar{p}} \right) dx dy dz &= - \iiint \frac{p'}{\bar{\rho}} \frac{\partial \bar{\rho} w'}{\partial z} dx dy dz \\ &- \iiint \frac{N^2}{g} p' w' dx dy dz \end{aligned} \quad (96)$$

Due to the periodicity in x direction the integral at right-hand side of equation(96) is zero, and the total energy in whole domain is conserved. However,



the column energy over  $z$  between zero and model top in a fixed  $(x,y)$  point changes with time. Therefore we use the variable  $\int(\frac{1}{2}\bar{\rho}|\vec{v}'|^2 + \frac{1}{2}\frac{c_p}{\bar{p}}\frac{p'^2}{\bar{p}})dz$  to describe the local difference between the time behavior of the stationary wave and its initial state.

The cases we chose are both the noninitialized and the initialized fields of  $\bar{u} = 25.m/s$ ,  $\bar{u} = -5.m/s$  and for wind shear(b), namely  $\bar{u}$  from  $-5.m/s$  at surface to  $25.m/s$  on the top.

Fig.15 shows the time evolutions of the column kinetic, internal and total energies at  $(0^\circ E, 45^\circ N)$  as compared to those at the initial state. It is found that in the mean flow of  $\bar{u} = 25.m/s$  the column energy changes around that at the initial state with the period about 18 days for the noninitialized field and 16 days for the initialized one. The maximum increase of the column energy of the stationary wave from its initial state is by 180% for the noninitialized field, while the maximum increase for the initialized field is smaller than that for the noninitialized one, namely 110%. On the other hand, at  $\bar{u} = -5.m/s$  for both the noninitialized and the initialized fields the maximum departure of the energy from its initial state is within 5%. However, in the case of shear(b) for both the noninitialized and the initialized fields the energy first jumps from the initial state to some level, and then oscillates around that level with the period of 3 to 4 days. The mean value of the energy oscillation is as about 4 to 5 times larger than the initial value.

Therefore, the above results suggest that in the presence of moderate westerlies, in which the planetary stationary waves are propagating, the fore-

casting error is large when a model lid is imposed. However, in the presence of easterlies the stationary waves are trapped, and the forecasting error is relatively small. This is because in the presence of westerlies the difference of the initial stationary waves with radiation condition and the model stationary wave is large, and so spurious Rossby wave is excited. The spurious Rossby wave travels around with time in the absence of damping. However, in the presence of easterlies the difference of the initial stationary waves and the model stationary waves is very small, and so the time behavior of the initial fields is near stationary. Moreover, the comparison of the noninitialized and the initialized cases indicates that initialization does not tend to change the major features of the forecasting errors resulted from the placement of the model lid.

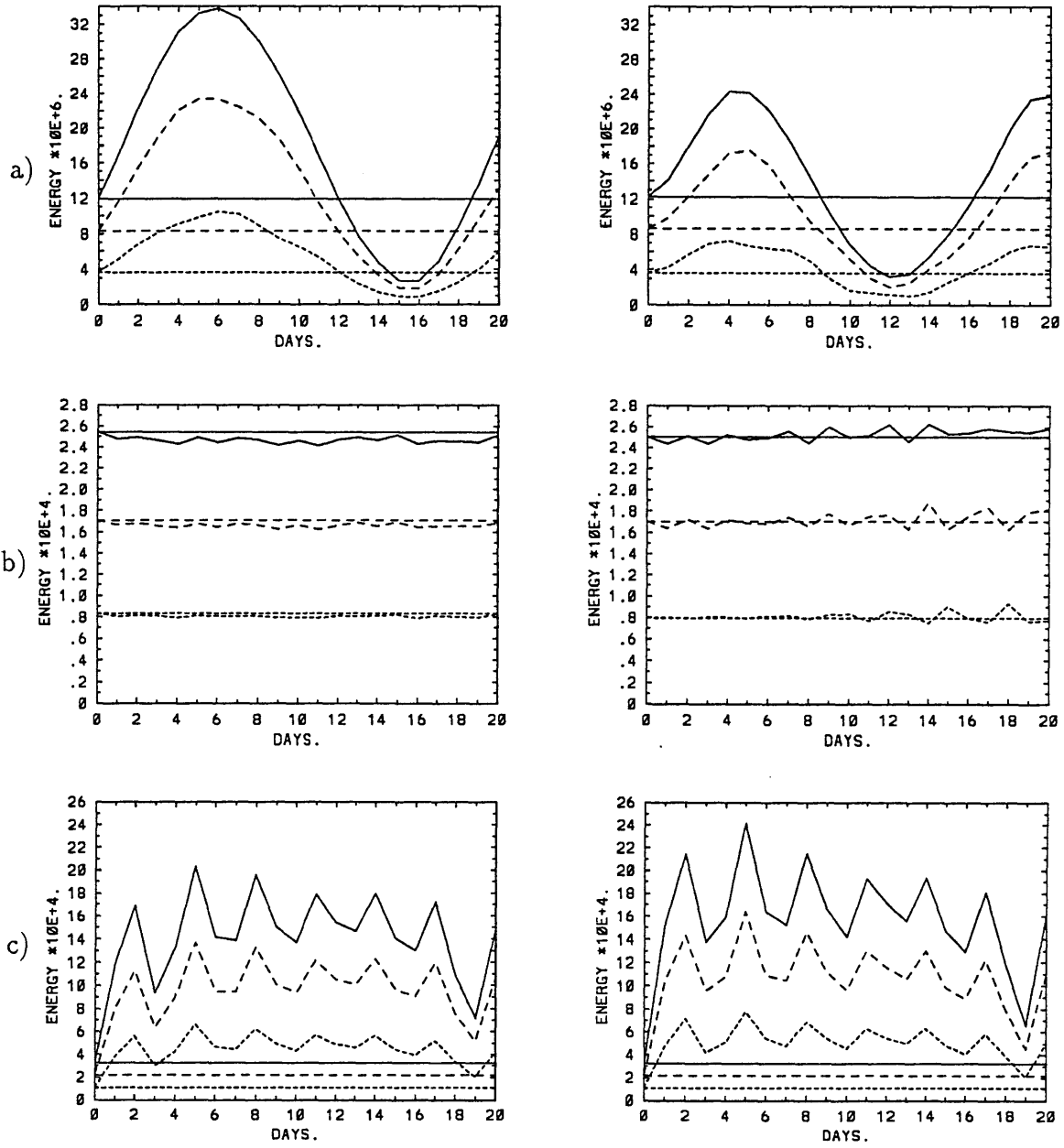


Figure 15: The change of column energy in  $J/m^2$  from day 0 to day 20. a):  $\bar{u} = 25.m/s$ , b):  $\bar{u} = -5.m/s$ , c): with wind shear(b). Solid line —: total energy, long dashed line-----: kinetic energy, short dashed line -----: internal energy. The horizontal lines are the initial values of energy as reference. Left: the noninitialied field, right: the initialized field.

## 7 Conclusion

Applying the normal mode initialization method to planetary stationary wave disturbances has been studied. It is found that the vertical modes for streamfunction  $\psi'$  and  $v'$  are good representations of the vertical structures of the initial fields varying in mean zonal flows. However, the mode structure of  $u'$  is heavily affected by NMI in the presence of easterlies. This is because eastward Rossby waves are absent in the eigenmodes of the normal mode initialization. Therefore, only in westerlies is the time behavior of the initialized field similar to that of the noninitialized one.

Furthermore, it is concluded that initialization is sensitive to mean zonal flow but not the existence of model lid. The change of mode structure by NMI strongly depends on mean zonal flow and this change is essential to the time behavior of stationary wave. However, the relevance of initialization to more realistic mean flows needs to be further investigated.

In addition, it is found that in the presence of moderate westerlies the error of forecasting stationary waves is large due to the placement of a model lid. Initialization, however, does not tend to change this feature. On the other hand, in easterlies the noninitialized fields behave like the original stationary waves and the forecasting errors are small.

## 8 References

- Arlindo M.DaSilva and Richard S. Lindzen**, 1987, A Mechanism for excitation of ultralong Rossby waves. *J.Atmos.Sci.*, 44, 3625-3639
- Arlindo M.DaSilva**, 1989, The role of temporal change of the wind on the excitation of large scale transients. Ph.D thesis, CMPO at M.I.T.
- Baumhefner, D., and P.Downey**, 1978, Forecast intercomparisons from three numerical weather prediction models. *Mon.Wea.Rev.*,106,1245-1279
- Charney, J.G. and P. G. Drazin**, 1969, Propagation of planetary scale disturbance from low into the upper atmosphere. *J.Geophys.Res.*, 66, 83-110
- Daley, R.**, 1981, Normal mode initialization. *Rev.Geophys.Space Phys.*, 19, 450-468
- Daley, R., J.Tribbia and D.Williamson**, 1981, The excitation of large-scale free Rossby waves in numerical weather prediction. *Mon.Wea.Rev.*, 109, 1836-1861
- Dickinson, R., and D.Williamson**, 1972, Free oscillations of a discrete stratified fluid with applications to numerical weather prediction. *J.Atmos.Sci.*, 29, 623-640

- Jacqmin, D., and R.S.Lindzen**, 1985, The causation and sensitivity of the northern winter planetary waves. *J.Atmos.Sci.*, 42, 724-745.
- Kasahara, A., and K.Puri** ,1981, Spectral representation of three dimensional global data by expansion in normal modes. *Mon.Wea.Rev.*, 109, 37-51
- Kasahara, A.**, 1976, Normal modes of untra-long waves in the atmosphere. *Mon.Wea.Rev.*, 104, 669-690
- Lambert, S., and P.Merilees**, 1978, A study of planetary wave errors in a spectral numerical weather prediction model. *Atmos.Ocean*, 16, 197-211
- Lindzen, R.S.**, 1967, Planetary waves on beta planes. *Mon.Wea.Rev.*, 94, 441-451
- Lindzen, R.S.**, 1968, Rossby waves with negative equivalent depths -comments on a note by G.A.Corby, *Quart.J.R.Met.Soc.*, 94
- Lindzen, R., B., Farrell and D.Jacqmin**, 1982, Vacillations due to wave interference: Application to the atmosphere and to analog experiments. *J. Atmos.Sci.*, 39, 14-23
- Lorenz, E.**, 1969, The predictability of a flow which possesses many scales of motion. *Tellus*, 21, 248-307

- Machenhauer, B.**, 1977, On the dynamics of gravity oscillations in a shallow water model with application to normal mode initialization. Beitr.Phys.Atmos., 50, 253-271
- Nigam,S. and R.S.Lindzen**, 1989, The sensitivity of stationary waves to variations in the basic state zonal flow. J.Atmos.Sci., 46, 1746-1768
- Philip Thompson**, 1987, Methods of suppressing gravity wave solutions: the relation between initialization and filtering.
- Somerville, R.**, 1980, Tropical influences on the predictability of ultralong waves. J.Atmos.Sci., 37, 1141-1156
- Williamson, D.L., and R.E.Dickinson**, 1976, Free oscillations of the NCAR global circulation model. Mon.Wea.Rev., 104, 1372-1391